

Industry 4.0 Adoption Using AI/ML Driven Metamodels for High-Performance Ductile Iron Sand Casting Design and Manufacturing

Jiten Shah

Product Development & Analysis (PDA) LLC, Naperville, Illinois, USA

Brian Began

American Foundry Society, Schaumburg, Illinois, USA

Copyright 2024 American Foundry Society

ABSTRACT

Data-centric near real-time intelligent process control for smart manufacturing in an Industry 4.0 era is of tremendous value. Design and manufacturing of high-performance ductile iron sand castings is a multi-variant complex process with much uncertainty involved. As a result, in spite of a well-controlled operation and an experienced workforce, iron foundries in a production environment do face sporadic shrinkage and lots with nonconforming property requirements, resulting in scrap or rework.

A framework and methodology consisting of AI (Artificial Intelligence) and ML (Machine Learning) tools, coupled with ICME (Integrated Computational Materials Engineering) and process simulation tools will be presented to quantify uncertainty (UQ). Metamodels, both predictive and prescriptive in near real-time were developed using such AI/ML techniques using historical production and selective Design of Experiments (DOE)-generated additional data. The data will be presented including details on successful corrective action production trials. The proposed framework and approach is applicable to solve such complex problems encountered in the foundry and machining operations where there is uncertainty.

Keywords: Artificial Intelligence, AI, Machine Learning, ML, Industry 4.0, metamodels, Uncertainty Quantification (UQ), Integrated Computational Materials Engineering, ICME, casting process simulation, smart manufacturing

INTRODUCTION

Metalcasting costs and lead times are severely impacted by scrap due to shrinkage and non-conformance of the properties. Occasionally, 100% X-ray inspections are required on some high-performance structural cast components due to the inability to reliably predict internal soundness, which in turn detrimentally impacts the cost and lead time as well. Typically, in production, after scrap is realized, root cause analysis is performed by examining

the recent lot process data coupled with prior knowledge and experience. Subsequently, corrective actions are taken to mitigate the scrap in subsequent campaigns. These corrective actions are disruptive and don't always resolve the issues, due (at times) to the seemingly insurmountable list of key variables and the uncertainty associated with many of them

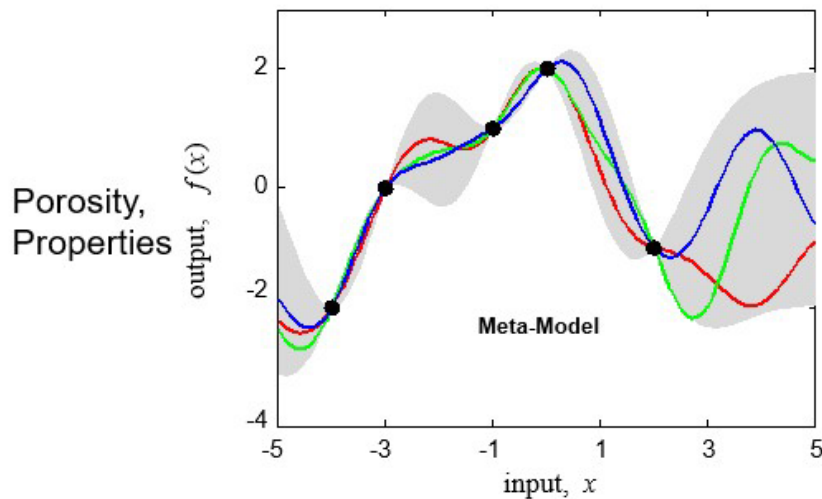
In an Industry 4.0 environment, key process data from design to the final inspection are captured digitally and stored. Metamodels, also known as algorithms or emulators, derived from these digital historical data, using AI/ML techniques predict the result of a multiplicity of variable interactions in near real-time and accordingly can assist with corrective action options.¹

Integrated Computational Materials Engineering (ICME), also known as Casting Process Simulation or Modeling, has been a very effective, mature, and widely used physics-based computer simulation tool used in industry. It is used to reliably predict shrinkage porosity and other filling- and solidification-related defects as well as to predict microstructure and mechanical properties in various iron and aluminum alloys over the spectrum of casting processes and varying mold media.

However, ICME is predominantly used at the design and new product process development stage and is very effective in conducting the root cause postmortem analysis to eliminate scrap in the production environment. ICME considers a finite set of variables, and it is not plausible as a near real-time decision-making tool for situational guidance. The accuracy of prediction with ICME is very high; hence, it should play an important role in integrating with a proper metamodel development process. In this project, it was extensively used for metamodel calibration, verification, and validation for two demonstration military cast components as well as DOE trial test casting shapes.

A metamodel is an analysis, construction, and development of the frames, rules, constraints, integrated ICME model outputs, and theories applicable and useful for modeling a predefined class of problems. A demonstration 100-70-03 grade of sand cast ductile iron military part in production since 2012 exhibited sporadic shrinkage at riser contacts that were seen visually and occasionally did not meet the desired minimum as-cast

yield strength property. Figure 1 depicts response variables (shrinkage porosity and as-cast yield strength values) as an output and all variables listed as parameters; blue line indicates the actual results; red line is the predictive model without uncertainty and green line indicates metamodel with uncertainty quantified (UQ), bringing the predictions closer to the reality and reducing the error (i.e., the gap).



Parameters – chemistry, pour temp. & time, mold material, section thickness, riser type, melt charge composition, etc.

Figure 1. Metamodel depiction of response variables.

Figure 2 illustrates the framework developed and proposed for metamodel development within any alloy or casting process. An extensive amount of time and effort were spent in the data mining phase for data set #1 from Foundry A. All the historical digital data for the demonstration part going back to 2012 (over 66 lots/campaigns) was collected, verified, and organized on a time sequence basis. When data was missing, these lots were addressed statistically. The objective functions were to minimize or eliminate shrinkage and maximize the as-cast yield strength property. As shown in Figure 3, data from various silos (molding sand, furnace charge, pour temperature, pouring time, final spectrochemical analysis including all trace elements, microstructural and mechanical properties) was collected and consolidated into a single Excel file.

The shrinkage was reported per lot as a percentage of the total scrap and the number of pieces produced per lot. Castings were not serialized in production, so no one-to-one traceability was available. Controlled production runs were witnessed, and additional observational data was collected and verified with the automated collected data. During this exercise, pour time measurements were identified as one of the uncertainties. Additional uncertainty was assumed to be mold hardness (soft vs. hard) and riser sleeve compression (100% vs. 70%, as shown in Figure 4), which were not measured in production, so additional data had to be generated by conducting a series of DOE-based controlled casting trials in a laboratory environment.

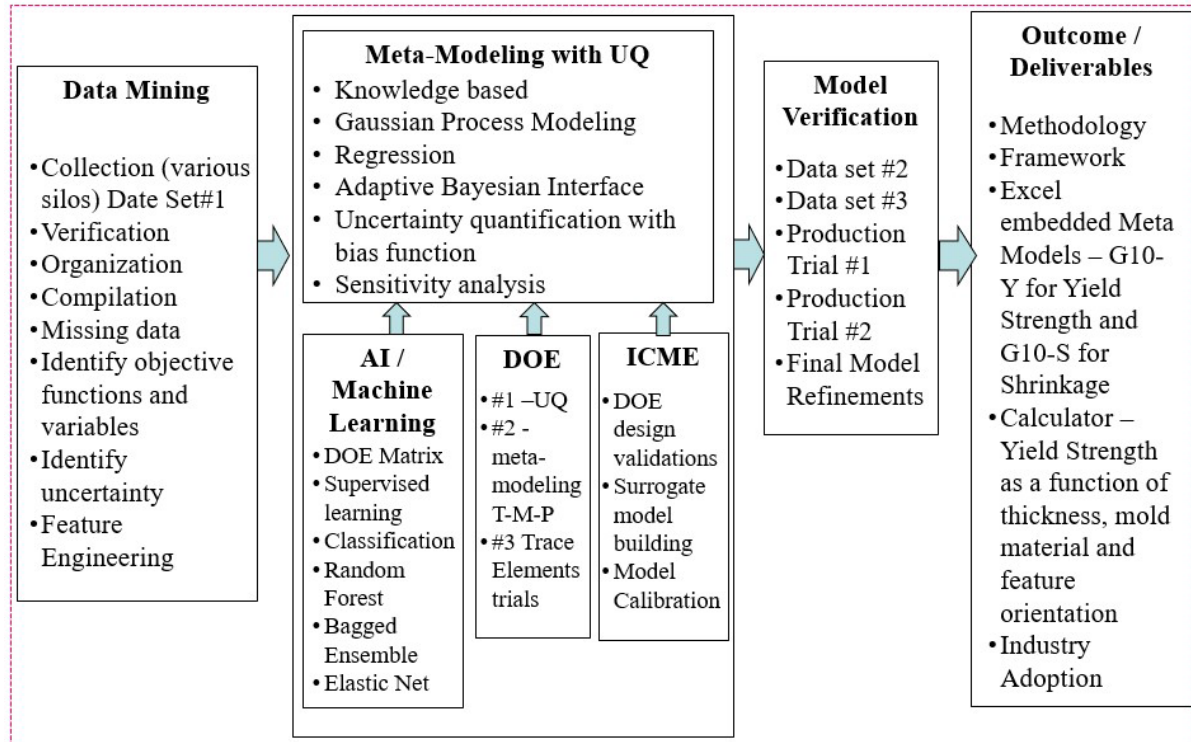


Figure 2. The metamodel development framework.

| READY | | | | | | | | | | | | | | | | |
|-------|---------|----------|-----------|--------|---------|------------|-----------|-------------------|----------------|--------|-------|--------|-------|-------|-------|------|
| | A | B | C | D | E | F | G | H | I | J | K | L | M | N | O | P |
| 1 | Date | ScrapPct | ShrinkPct | PourWt | PourSec | PourWt2Rev | PourTemp2 | TotPourWtPerLadle | ChargeScrapPct | MeltCE | MeltC | FinAF1 | FinFe | RevSi | FinMn | FinP |
| 113 | 8/24/17 | 0.16935 | 0 | 54.5 | 9.3 | 671 | 2556 | 671 | 0.397250859 | 4.29 | 3.76 | | | | | |
| 114 | 8/24/17 | 0.16935 | 0 | 55 | 8 | 671 | 2556 | 671 | 0.397250859 | 4.29 | 3.76 | | | | | |

Figure 3. Various data silos of historical data for the demonstration part (Data Set #1 from Foundry A).

Artificial Intelligence (AI) is a study of the intelligent agents/factors of a complex system that perceives its environment and takes actions that maximize the chance of achieving its goals. To solve these problems, AI researchers have adapted and integrated a wide range of problem-solving techniques (i.e., machine learning algorithms based on data mining of historical select data searches, mathematical optimization, and methods based on statistics & probability). Machine Learning (ML) techniques are used to create knowledge from the historical data mined/collected to gain a deeper understanding of the casting manufacturing process and to short list the key influential parameters. The outcomes boost the confidence of key decision making in near real time. Various machine algorithms were developed as listed in Figure 2.

Uncertainty Quantification (UQ) is the science of quantifying, characterizing, tracing, and managing uncertainty in computational and ductile iron production systems. UQ seeks to address the problems associated with incorporating real-world process variability and probabilistic behavior into intelligent manufacturing. Casting simulations (ICME) answer the question: What will happen when the system is subjected to a single set of inputs? UQ expands on this question and asks: What is likely to happen when the system is subjected to a range of uncertain and variable inputs: mold hardness, riser sleeve compression, % steel scrap, pouring temperature and time, iron treatment and inoculation, etc.

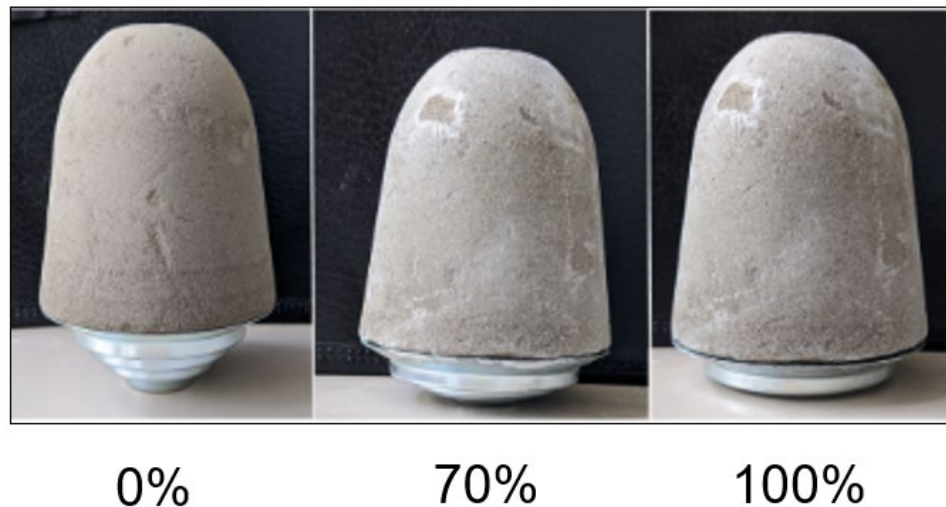
In this project, metamodeling with UQ was conducted using various approaches (Figure 2) and consisted of primarily three data sets:

- AI/ML-driven algorithms to analyze historical data and shortlist the key variables from over 55 variables based on the sensitivity.
- DOE-generated experimental data with uncertain variables (mold hardness, sleeve compression) coupled with historical data range of chemistry and other process parameters.

- The ICME generated data for surrogate model building, model calibration, and verification.

SLHS (Sliced Latin Hypercube Sampling) and OLHS (Optimized Latin Hypercube Sampling) statistical methods^{2,3,4} for generating a near-random sample of parameter values from a multidimensional distribution were used to create DOE samples for all controlled casting experiments (DOE #1 and DOE #2) as well as for the ICME runs to generate additional data for metamodeling with UQ.

Figure 4. Riser sleeve compression as an uncertain variable (100% vs. 70%).



EXPERIMENTAL PROCEDURE

DATA MINING

Data set #1 from Foundry A entailed over 66 production lots of a military demonstration part sand cast in 100-70-03 grade ductile iron. The part had been in production from 2012 through 2022, when the metamodel was developed. An average of 100 castings were poured in each lot and each contained data for 55 variables that were analyzed during the metamodeling development work. The response variables (i.e., scrap due to shrinkage and as-cast yield strength from the separately cast test bar of 1-in. cross section) were reported for each production lot. A few controlled production trials were run where castings were serialized for individual traceability so as to track pour temperature and pour

time to be used as verified system-recorded data. Individual castings were visually inspected for shrinkage at the riser contact and the risers were sectioned and measured for shrinkage volume. It was noted that most of the riser sleeve heights were found to be nearly 100% compressed so sleeve compression was flagged as another uncertain variable. A few sound castings were X-rayed to ensure that no internal shrinkage was seen. Pour time variability, due to measurement errors, was identified as uncertainty since actual measured values had less scatter than reported in historical data. Mold hardness, both on the horizontal as well as parting surfaces, were measured manually during various control production runs and were found to be highly variable, potentially leading to sporadic shrinkage. Hence, mold hardness was included as an uncertain variable. Unfortunately, no historical data was

measured or available for the mold hardness or actual riser sleeve compression percent.

For Data set #2, historical data was secured from the same various areas as previously mentioned; although, data in the form of 100% X-ray films to assess the level of shrinkage seen in the castings was also available/included. The X-ray data was secured from three critical areas labeled V1, V2 and V3 for

over 50 lots of the subject demonstration part. This part, run at Foundry B since 2018, uses a two-cavity pattern, with an Isocure core, on a high-pressure green sand molding line. The part experienced sporadic shrinkage beyond the acceptable X-ray Level 2 threshold, generating scrap and requiring 100% radiographic inspection. Figure 5 shows X-ray data from the first seven months of 2021.

| | CastDate | Pour Temp - Deg F | X-Ray Level Ratings | | | | | | Overall |
|-------|-----------------|----------------------|---------------------|------|------|----------|------|------|---------|
| | | | Cavity 1 | | | Cavity 2 | | | |
| | | | V1 | V2 | V3 | V1 | V2 | V3 | |
| V05 → | 1/7/2021 11:05 | N/A | N/A | N/A | N/A | N/A | N/A | N/A | |
| | 1/28/2021 15:54 | 2495 | 1.50 | 1.75 | 2.00 | 1.50 | 1.50 | 2.00 | 1.71 |
| | 2/25/2021 11:30 | 2493 | 1.46 | 1.14 | 1.45 | 1.91 | 1.18 | 1.55 | 1.45 |
| | 3/25/2021 19:12 | 2495 | 2.33 | 1.50 | 2.00 | 1.75 | 2.00 | 2.00 | 1.93 |
| | 5/13/2021 12:19 | 2512 | 3.00 | 1.50 | 2.00 | 2.50 | 1.00 | 2.00 | 2.00 |
| | 5/13/2021 12:41 | 2492 | 3.00 | 1.50 | 2.00 | 2.50 | 1.00 | 2.00 | 2.00 |
| | 5/13/2021 12:57 | 2486 | 2.00 | 1.50 | 2.00 | 1.50 | 1.50 | 2.00 | 1.75 |
| | 5/13/2021 13:36 | 2467 | 2.00 | 1.50 | 2.00 | 1.50 | 1.50 | 2.00 | 1.75 |
| | 5/19/2021 13:30 | 2495 | 2.17 | 1.50 | 2.33 | 1.83 | 1.67 | 2.00 | 1.92 |
| | 5/19/2021 13:45 | 2495 | 1.67 | 1.50 | 2.00 | 1.50 | 1.17 | 2.00 | 1.64 |
| | 5/19/2021 14:07 | 2465 | 2.17 | 1.67 | 2.00 | 1.67 | 1.50 | 2.00 | 1.84 |
| | 5/19/2021 14:28 | 2455 | 2.25 | 1.50 | 2.00 | 1.75 | 1.50 | 2.00 | 1.83 |
| V04 → | 7/15/2021 13:45 | 2467 | 2.00 | 1.00 | 1.50 | 1.50 | 1.00 | 1.67 | 1.45 |
| | 7/15/2021 14:02 | 2484 | 1.50 | 1.00 | 1.50 | 1.50 | 1.33 | 1.67 | 1.42 |
| | 7/15/2021 14:21 | 2500 | 1.50 | 1.75 | 1.50 | 1.50 | 1.00 | 1.33 | 1.43 |
| | 7/15/2021 14:49 | 2527 | 1.50 | 1.00 | 2.00 | 1.38 | 1.00 | 1.80 | 1.45 |

Figure 5. Summary of 100% X-ray readings for the second demonstration part during the first seven months of 2021.

The data maps the average shrinkage level seen in both cavities for each of the three zones. The overall numeric average of 1.7 was used as the metamodel threshold, meaning, any average shrinkage score of 1.7 and higher was defined as unacceptable and any score less than 1.7 was deemed acceptable.

Accordingly, the V05 condition was defined as the worst case while the V04 condition was defined as the best case. These conditions were analyzed using ICME-based simulation and using metamodel guided outputs before the production trials were conducted.

METAMODEL DEVELOPMENT WITH UQ

Figure 6 summarizes the design optimization framework for casting process metamodeling. Using data collected from historical foundry records and new experiments, two ML metamodels were created, one predicting as-cast yield strength (G10Y), another predicting shrinkage (G10S), from chemistry and processing conditions. With the two metamodels, casting processes were optimized with strength as a primary objective property, and no shrinkage as a constraint, subject to tradeoff between them and a combined metamodel (G10YS) was developed.

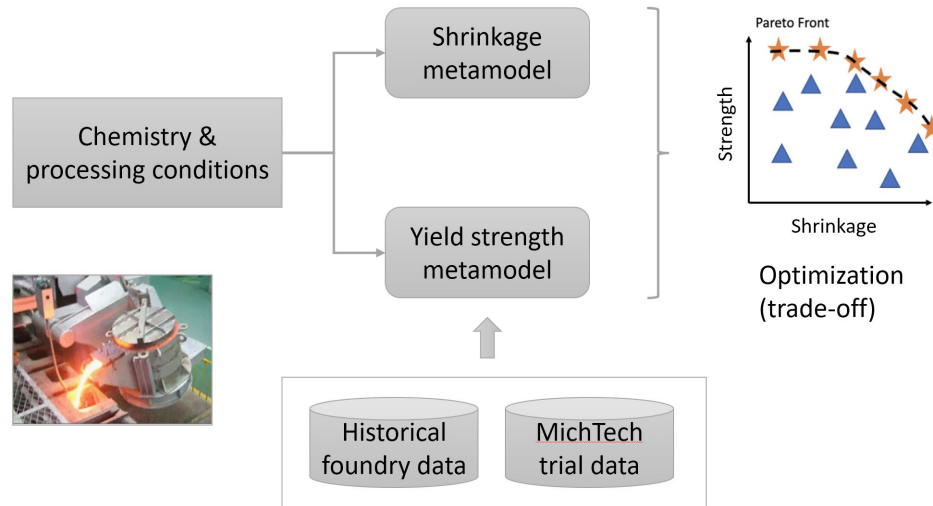


Figure 6. The ICME framework for casting process optimization.

The historical data had many missing values; hence, data cleaning was required. Mainly two approaches were taken: (1) for variables with many missing values, or not important for the target property based on expert's domain knowledge, the variables are discarded. (2) Imputation is performed for other variables with missing values, i.e., missing values are replaced by the mean value of all available records.

There is also a mismatch between historical and new data: some variables are involved in data from one source but not from another. In this case, two solutions were used: (1) treat the variable as one with missing data, and (2) create a model using the variables with complete data, and then create a "bias correction" model for the left-out variables, then combine the models.

The ML models explored included: (extended) linear models, tree-based models, ensemble models, and Gaussian process models. Linear models assume a linear correlation between the target property y (e.g., as-cast yield strength), and the predictors $X = [x_1, x_2, \dots]$ (e.g., chemistry): $y = X\beta$, and finds the optimal coefficients $\hat{\beta}$. It is deterministic and have physically meaningful interpretations. There are modifications that extend the capability of linear models. One extension is adding degree of polynomials (i.e., including x_i^2, x_i^3, \dots) and interactions (i.e., including terms like x_1x_2). This

allows the model to capture relations beyond linearity. Another extension is to add regularization. In this case, the training objective becomes:

$$\hat{\beta} = \arg \min_{\beta} (\|y - X\beta\|_2^2 + \lambda_1 \|\beta\|_1 + \lambda_2 \|\beta\|_2^2)$$

Where: $\|\cdot\|_n$ represents the L-n norm; the last two terms are regularization terms. With $\lambda_2 = 0$ and nonzero λ_1 , the model is a Lasso regression model,⁵ which generally produces "sparse" coefficients, i.e., coefficients for many variables are 0. It is therefore powerful for variable selection, specifically, it selects the predictors that have linear effects on the response. On the other hand, with $\lambda_1 = 0$ and nonzero λ_2 , the model is ridge regression,⁶ which is useful for shrinking the coefficients to avoid overfitting. With both terms nonzero, the elastic net model⁷ is obtained, which combines both methods merits.

A tree model⁸ works by making separations on predictor values, for which a decision tree is a prominent example. A decision tree is also useful for variable selection, especially variables with nonlinear effects on the response. While tree models are found not to be appropriate for our problem, they form the basis of most widely used ensemble models, random forest⁹ and gradient boosting.¹⁰ Both models train many decision trees as "base learners" and combine them to make a prediction. Ensemble models usually

require a large amount of training data to gain good performance. Once a good model is trained, tools such as Accumulated Local Effects (ALE) plots¹¹ can be used to extract information about variable importance and interactions therefrom.

Gaussian process (GP) modeling¹² assumes a joint Gaussian distribution between response y values at different X 's. The covariance of the distribution is inferred from the distance between X values via a kernel function. In addition to a predicted value, GP model also gives the variance associated y while giving predictions for new input x' . This enables uncertainty quantification (UQ),¹³ which is useful for experimental design,¹⁴ adaptive design optimization,¹⁵ and model calibration.¹⁶ In this project, because of the data sparsity, lack of data will be the main source of uncertainty, therefore, GP-based UQ is not highly needed. Nonetheless, GP models with UQ capabilities are useful in a variety of materials and process design problems.

Assessment of a regression model (response is continuous, quantitative) is straightforward. The deviation of predicted response \hat{y} from true response y , by mean square error (MSE), root MSE (RMSE), coefficient of determination R^2 , and so on, were simply measured. While for a classification model (response is categorical, qualitative), other assessments are needed. They are based on quantities and the confusion matrix, illustrated in Figure 7. Generally, a binary classification model first computes a probability for one class, and then outputs a class prediction according to a threshold in probability. By adjusting the threshold, various classification results are obtained with different true positive rate (TPR) and false positive rate (FPR). Plotting these rates as a curve, the receiver operating characteristics (ROC) curve is obtained and the area under curve (AUC) is used for model assessment. An AUC ROC (receiver operator characteristic) over 0.8 usually indicates a good model. Besides, using the relevant quantities, other metrics such as sensitivity and specialty are derived. We use these as auxiliary assessments and will describe their meanings later in this document.

DOE IN CONTROL LABORATORY CASTING TRIALS

To quantify uncertainty, a series of controlled laboratory casting trials were conducted, and the data generated were used for probabilistic metamodel development. The chemistry and processing conditions form a high-dimensional parameter space. Through the experiments and simulations, we seek relations between these parameters and the outcomes of casting. However, the experiments and simulations are costly and time-consuming, making full coverage.

DOE #1

In DOE #1, an equivalent test plate casting with the same pour volume and maximum section thickness of 1" was designed and poured with the identical gating and riser sleeve as the demonstration part in production with sporadic shrinkage. Photos are provided in Figure 8. The test plate design was validated with the ICME tool to ensure the casting is predicted to be sound and to estimate the total shrinkage volume, microstructure, and properties at the test locations using various target chemistries. A series of ICME runs to build the surrogate model were conducted using SLHS (Sliced Latin Hypercube Sampling) based sampling and the input and output data generated were used for metamodel development. A total of 16 castings (eight heats of ductile iron grade 100-70-03 in the range of Foundry A's historical data) were poured in a laboratory-controlled environment, capturing all the variables as shown in Figure 9. Key variables were chemistry (carbon equivalent, CE), pour temperature, pour time, and furnace charge with % steel scrap. The key variables for uncertainty quantification were mold hardness (soft 85 and hard 95 on B scale) and riser sleeve compression (100% and 70%). The response variable and shrinkage volume were measured for every test casting by dunking the sample in water and using Archimedes principle to develop the input for the metamodel algorithm. Microstructure and mechanical properties were measured at known locations for ICME-based model calibration as well as metamodel algorithm development. Every plate and test specimen for various measurements was labeled for accurate traceability. Figure 10 shows the cutting plan for the various measurements taken.

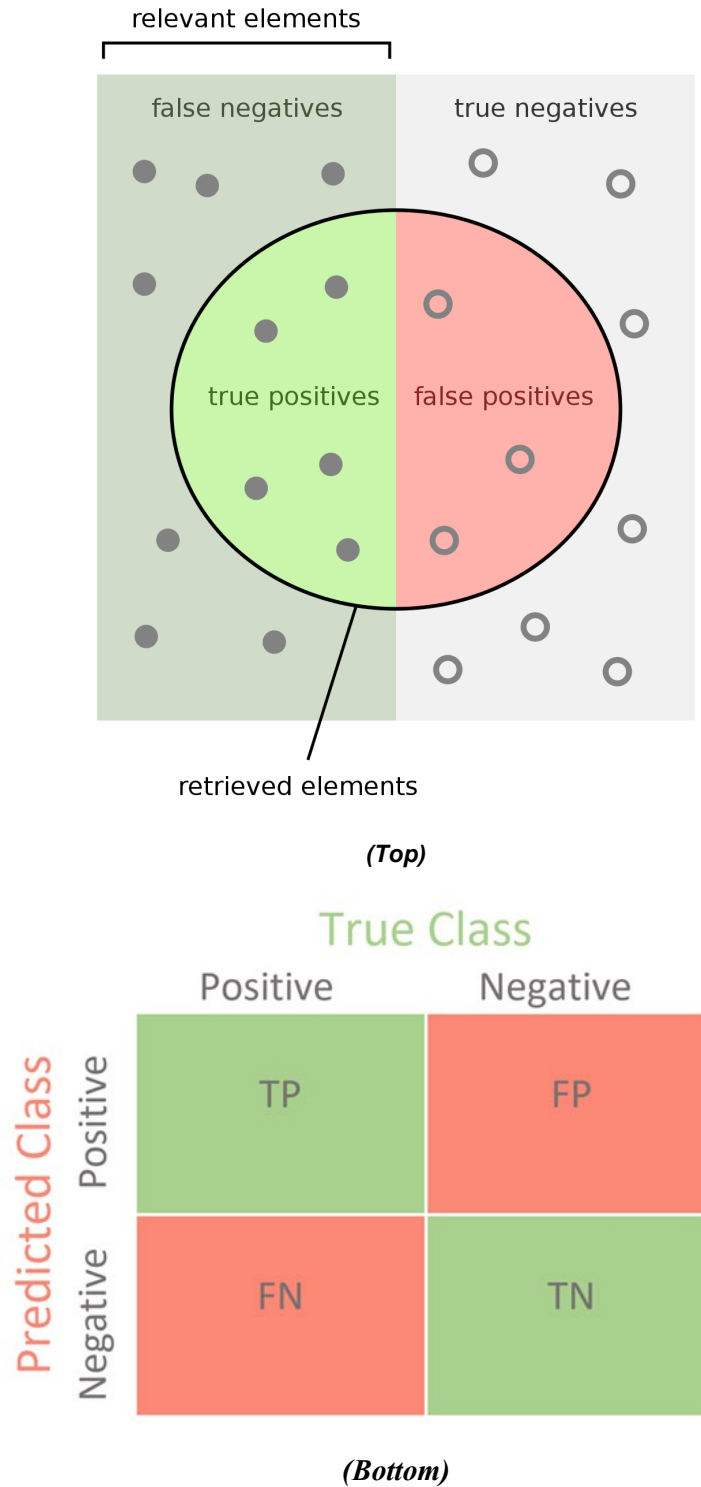


Figure 7. Top view: illustration of binary classification result and relevant quantities. Bottom view: the confusion matrix.



Figure 8. Test castings are poured (left view), a test plate casting with gating and sleeved riser (middle view), and shrinkage cavity in the riser (right view).

| Target Conditions DOE #1 | | | | | | Actual Conditions | | | | | | |
|--------------------------|------------------------|---------------|------|----------------------|------------------|-------------------|------------------------|---------------|------|-----------------------|------------------|---------------|
| Run # | Sleeve Compression (%) | Mold Hardness | CE | Pour Temperature (F) | Charge Scrap (%) | Run # | Sleeve Compression (%) | Mold Hardness | CE | Pour Temperature (F)* | Charge Scrap (%) | Pour Time (s) |
| 1 | 70 | 95 | 4.35 | 2500 | 40 | 1 | 70 | 94 | 4.36 | 2630 | 40 | 19 |
| 2 | 100 | 85 | 4.35 | 2500 | 40 | 2 | 100 | 86 | 4.36 | 2590 | 40 | 20 |
| 3 | 70 | 85 | 4.35 | 2600 | 40 | 3 | 70 | 87 | 4.36 | 2490 | 40 | 15 |
| 4 | 100 | 95 | 4.35 | 2600 | 40 | 4 | 100 | 95 | 4.36 | 2470 | 40 | 18 |
| 5 | 70 | 85 | 4.6 | 2600 | 40 | 5 | 70 | 89 | 4.62 | 2660 | 40 | 16 |
| 6 | 100 | 95 | 4.6 | 2600 | 40 | 6 | 100 | 95 | 4.62 | 2620 | 40 | 17 |
| 7 | 70 | 95 | 4.6 | 2500 | 40 | 7 | 70 | 97 | 4.62 | 2510 | 40 | 19 |
| 8 | 100 | 85 | 4.6 | 2500 | 40 | 8 | 100 | 84 | 4.62 | 2460 | 40 | 13 |
| 9 | 70 | 85 | 4.35 | 2600 | 60 | 9 | 70 | 85 | 4.35 | 2660 | 60 | 18 |
| 10 | 100 | 95 | 4.35 | 2600 | 60 | 10 | 100 | 95 | 4.35 | 2640 | 60 | 17 |
| 11 | 70 | 95 | 4.35 | 2500 | 60 | 11 | 70 | 95 | 4.35 | 2590 | 60 | 17 |
| 12 | 100 | 85 | 4.35 | 2500 | 60 | 12 | 100 | 85 | 4.35 | 2570 | 60 | 12 |
| 13 | 70 | 95 | 4.6 | 2600 | 60 | 13 | 70 | 95 | 4.6 | 2640 | 61 | 16 |
| 14 | 100 | 85 | 4.6 | 2600 | 60 | 14 | 100 | 85 | 4.6 | 2530 | 61 | 15 |
| 15 | 70 | 85 | 4.6 | 2500 | 60 | 15 | 70 | 85 | 4.6 | 2450 | 61 | 15 |
| 16 | 100 | 95 | 4.6 | 2500 | 60 | 16 | 100 | 95 | 4.6 | 2420 | 61 | 14 |

*Any castings highlighted in gray were re-cast

Figure 9. DOE #1 test conditions show the target conditions vs. actual pour conditions.

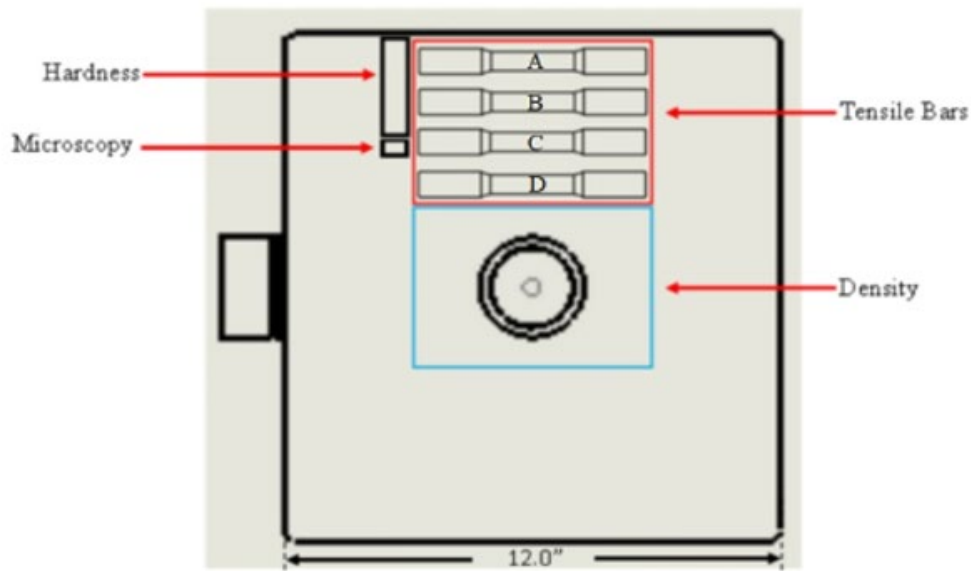


Figure 10. DOE #1 test plate sectioning layout for microstructure, properties and density measurements.

DOE #2

Similarly, step plates (mimicking horizontal casting orientation) and finger plates (mimicking vertically-parted casting orientation) with varying thicknesses of 0.5, 0.875, 1, and 1.5-in. were designed and validated by ICME-based casting process simulation to ensure sound castings and to predict microstructure and properties at the test locations for the various mold materials (green sand–soft & hard, chemically bonded/no-bake, 3D printed ceramic and hybrid of green sand with no-bake to simulate cored cast parts), chemistry, pour temperature and pour time combinations.

Sampling was developed using the OLHS method for various ICME simulations to generate data to build the metamodel for the as-cast yield strength as a function of section thickness, mold materials, and casting orientation for the benefit of the design and foundry engineers.

Both casting types had section thicknesses of 0.5, 0.875, 1.0, and 1.5-inch. Microscopy, Brinell hardness, and tensile testing samples were sectioned from each of these thickness per casting using a bandsaw (Figure 11).

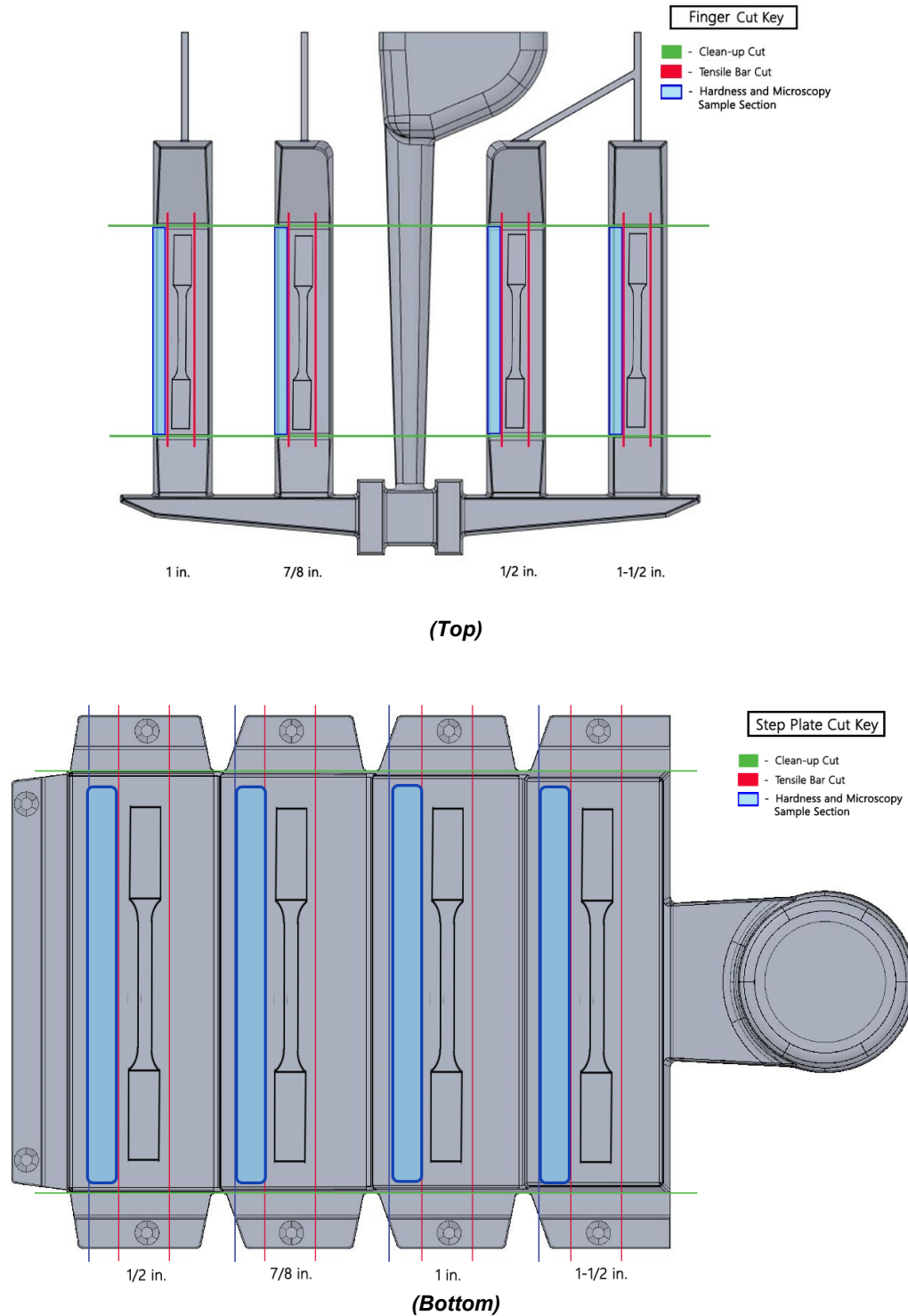


Figure 11. Diagrams show the locations that microscopy, hardness, and tensile samples were sectioned from the finger castings (top) and step-plate (bottom) castings.

All heats were made up of 40% ductile iron returns, 30% steel scrap, and 30% pig iron. All heats were poured at the target superheat temperature of $2600\text{F} \pm 100\text{F}$ ($1427\text{C} \pm 55.6\text{C}$). Thermocouples were used to record the cooling of both the metal and mold of each casting. Mold temperatures were taken $\frac{1}{8}$ " away from the surface of the center of the 0.5" section on all castings. Metal temperatures were measured

through the runner and riser systems of the finger and step-plate castings (Figure 12). ICME-based simulation key boundary conditions were validated by comparing the predicted cooling curves vs. actual curves obtained with thermocouple reading as shown in Figure 13.

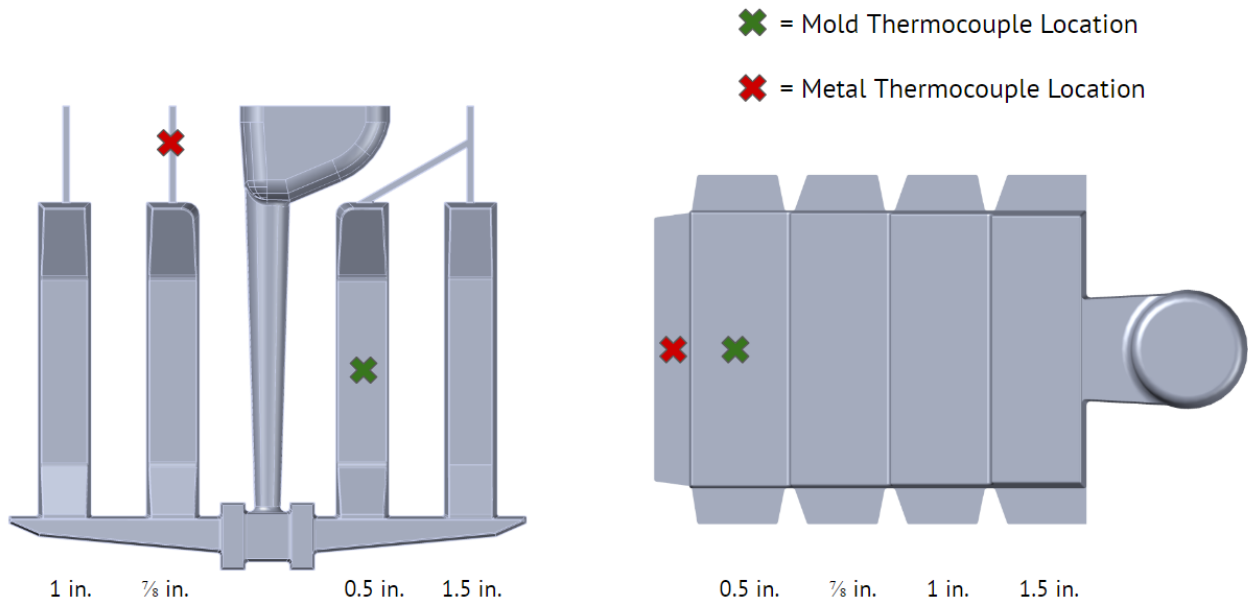
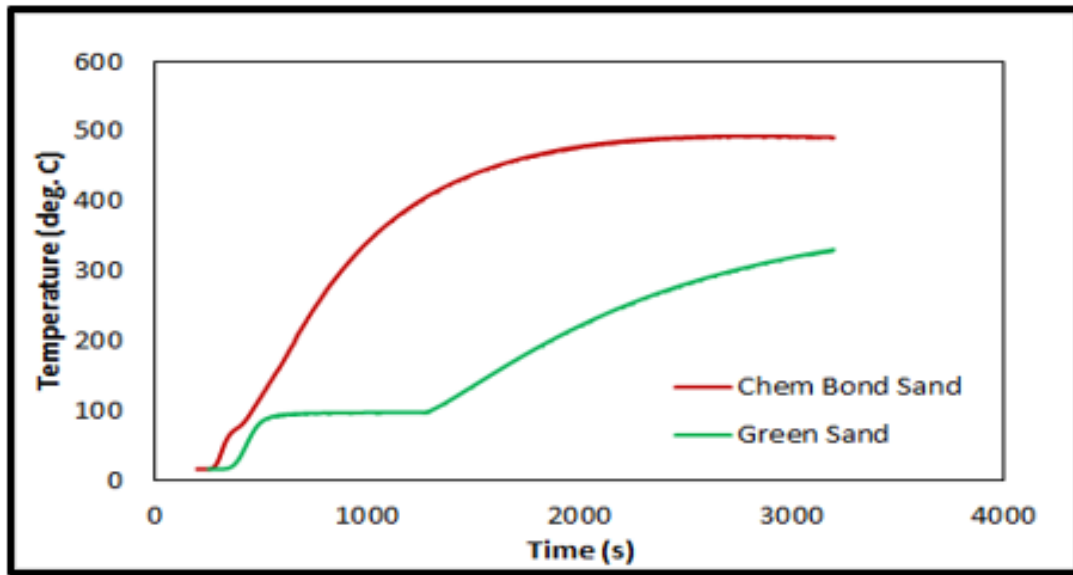
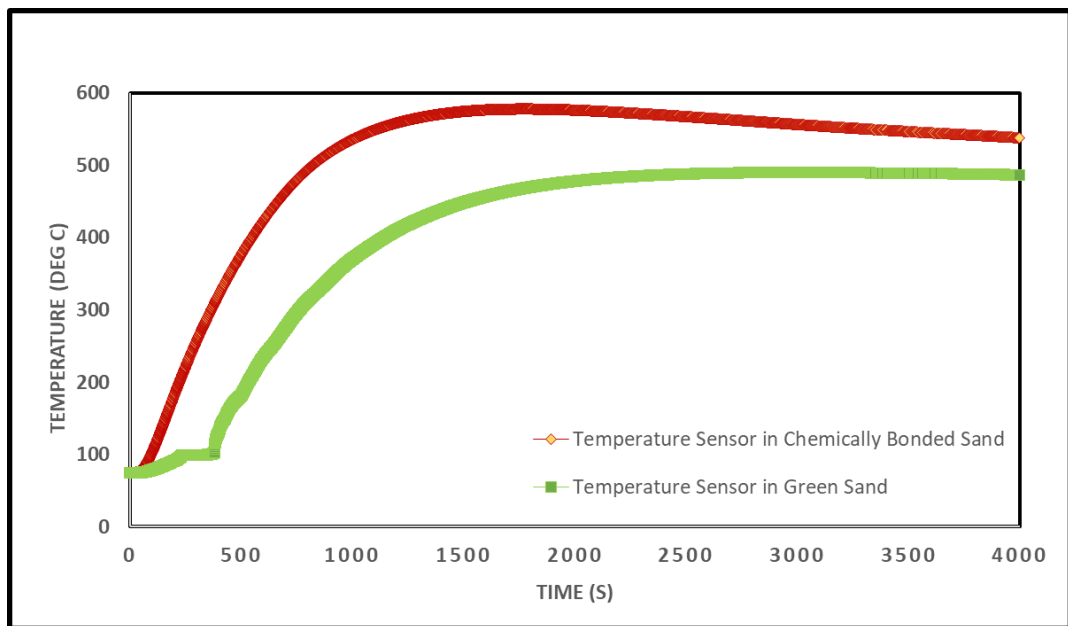


Figure 12. Metal (red) and mold (green) thermocouple locations for finger and step-plate castings.

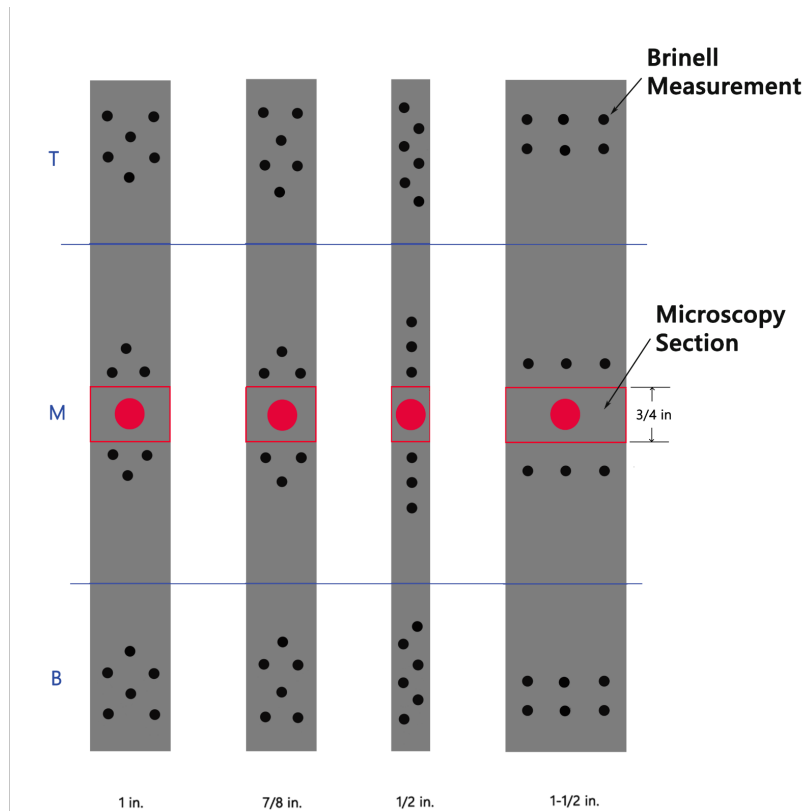


Actual thermocouple data

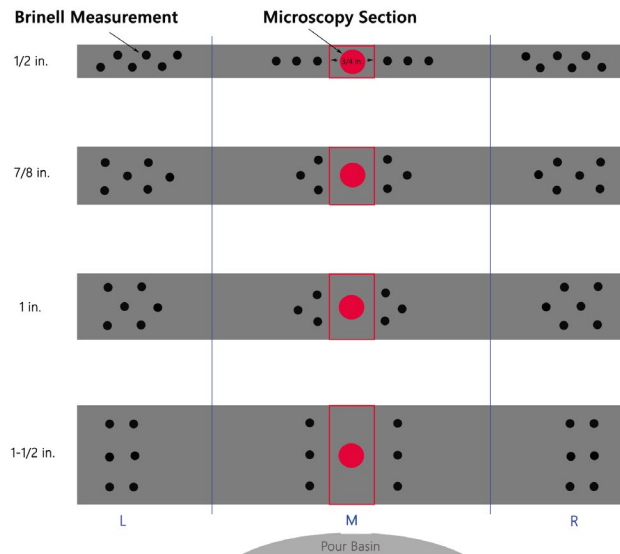


Simulated cooling curves

Figure 13. Comparison between actual thermocouple data (top) vs. simulated cooling curves (bottom) at select locations.



(Top)



(Bottom)

Figure 14. Brinell hardness measurement locations for finger and step-plate sections. Centers of sections were removed and used for microscopy samples.

BRINELL HARDNESS

Brinell hardness with a standard 10 mm spherical indenter tip and a 3000 kgf load was measured for each section thickness from each casting HRB scale. Measurements were taken across the entire length of sections (Figure 14). Six measurements were taken at each top, middle, and bottom of the finger castings and per the left, middle, and right of the step-plates. The hardness and indent diameter were measured using a Biological Optic Sensing System (BOSS) imaging system. All of the data generated was used in the development of the metamodel.

METALLOGRAPHY

All metallography samples were mounted in 1.25" epoxy molds and polished using a LECO 9-mount auto polisher. All samples were etched with 3% Nital for 5 seconds prior to imaging. Four images per sample condition were analyzed using the Olympus Stream Software. The "Cast Iron" material analysis feature was used to determine graphite nodule size and nodularity. Due to the low volume fraction of ferrite in a majority of the sample's microstructure, manual point counting was used to measure volume fraction of ferrite following procedures outlined in ASTM-E562.

TENSILE TESTING

For the section thicknesses of 0.875, 1.0, and 1.5," ASTM Standard E8 Specimen Type 1 round tensile bars with a gauge cross-section diameter of 0.5" were machined. For the 0.5" thick sections, ASTM Standard E8 Specimen Type 3 round tensile bars with a gauge cross-section diameter of 0.25" were machined. The as-cast yield strength, tensile strength, and elongation were measured using an Instron 4206

mechanical testing machine in conjunction with MTS Test Works software. (2" and 1" extensometers were used specifically to measure elongation for sample Type 1 and Type 3, respectively.) A 30,000 lb. load cell was used for all tensile tests.

DOE #3

Based on the preliminary metamodel development, some of the trace elements indicated noticeable impact on the as-cast yield strength as well as shrinkage inducement tendency. Hence, to validate the metamodel output, DOE #3 was planned and a total of 3 heats were poured.

ICME WORK

Extensive ICME-based casting process modeling by simulating filling, solidification & cooling, and microstructure properties evolution were conducted for the two demonstration military articles as well as all DOE #1 and #2 test castings. Figure 15 shows a typical output for DOE #1 from the ICME-based casting process simulation of the test plate; feed volume, and predicted properties data were used for the metamodel development and calibration. For Foundry B's demonstration article, ICME-based predictions to reduce the shrinkage severity from Level 3 to Level 2 using metamodel-predicted adjustments were conducted. Typical ICME output results are shown in Figure 16 for DOE #2 test castings (step plate and finger vertical test plates in section thickness of 0.5, 0.875, 1, and 1.5-in.). A series of ICME runs to build the surrogate model were conducted using SLHS (Sliced Latin Hypercube Sampling) and OLHS (Optimized Latin Hypercube Sampling) based sampling and the input and output data generated were used for the metamodel development.

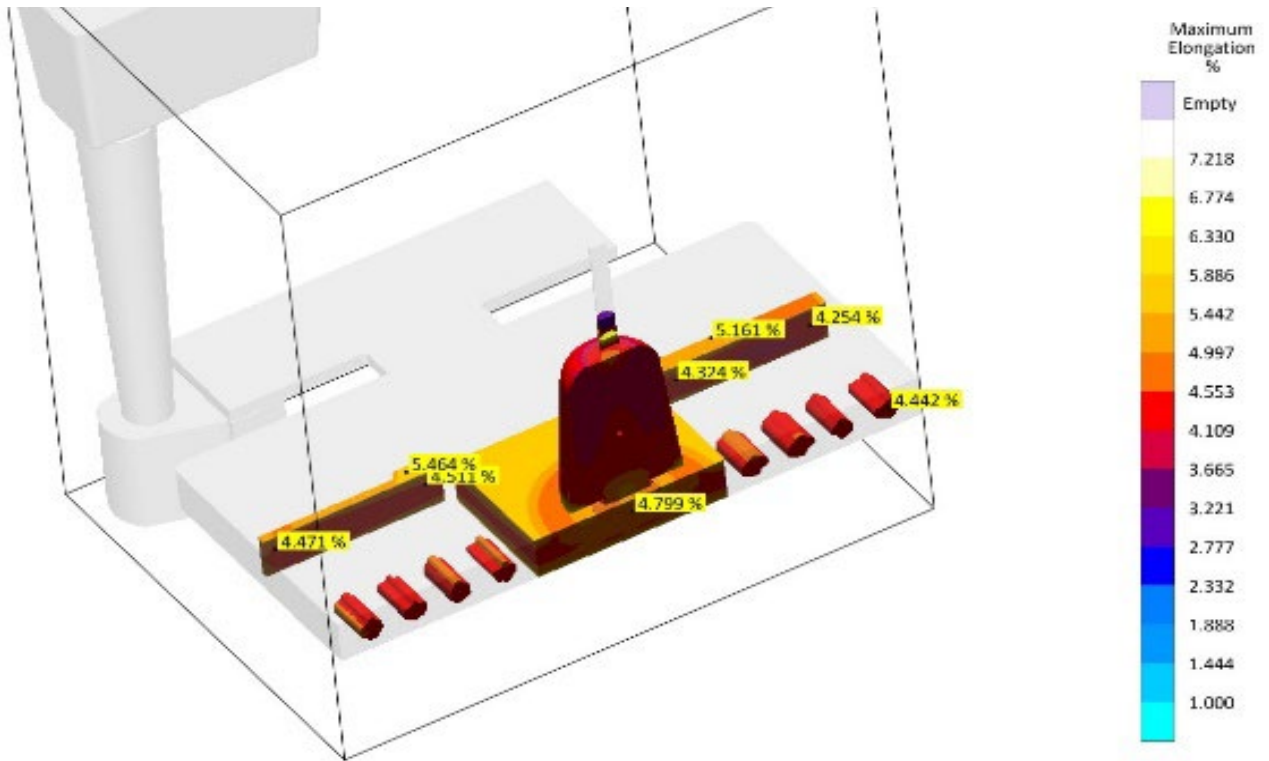


Figure 15. ICME output for DOE #1 test plate predicting local properties at test bar locations.

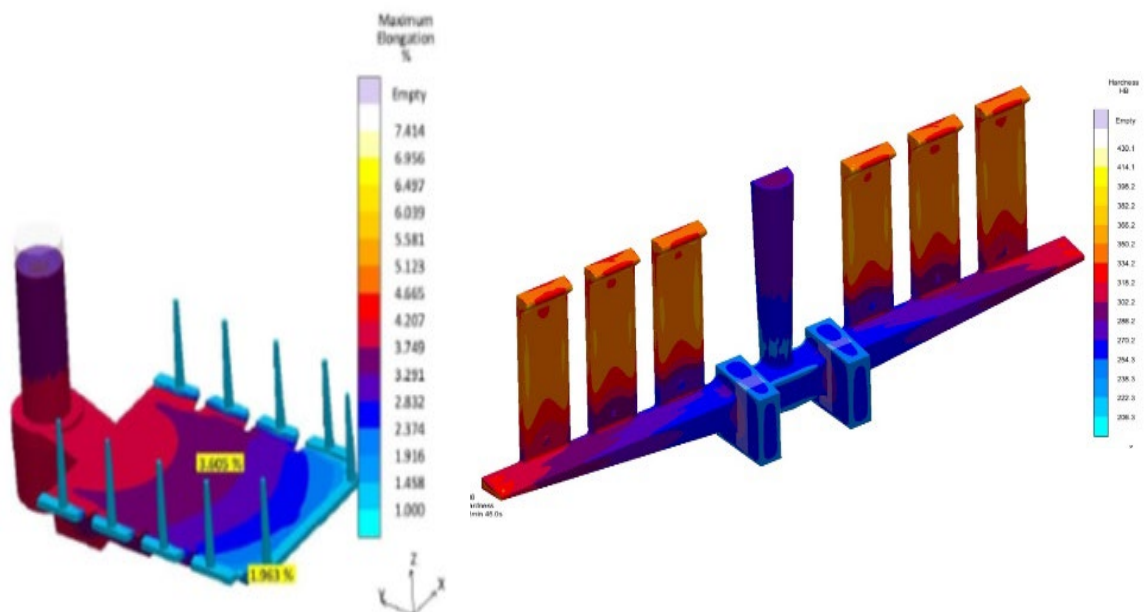


Figure 16. ICME output for DOE #2 step plate and vertical finger test plates (0.5, 0.875, 1 and 1.5-in. thicknesses each).

RESULTS AND DISCUSSION

DOE #1 RESULTS

All 16 castings with risers were sectioned and the riser shrinkage volume was measured for each. Microstructure and various mechanical properties were measured off the cut-out specimens from every test plate casting per the layout shown in Figure 10. Table 1 shows the summary of the results. The values reported were the average from multiple specimens

measured at the same locations (i.e., four density measurements; five hardness and microstructure measurements; four as-cast yield strength, ultimate tensile strength, and elongation measurements) for a total exceeding 800 measurements were recorded for the entire campaign and used for the metamodel development.

Table 1. Summary of Inputs and Outputs for DOE #1

| Plate Number | Sleeve Compression (%) | Mold Hardness | Pour Temperature (F) | Charge Returns (%) | Pour Time (s) | Avg. Thickness (in.) | Heat Number | CE | Material Fed into Casting (lb) | Pearlite (%) | Yield Strength (psi) | Tensile Strength (PSI) | Elongation (%) | Elastic Modulus (psi) | Avg Brinell Hardness (BHN) |
|--------------|------------------------|---------------|----------------------|--------------------|---------------|----------------------|-------------|-----------|--------------------------------|--------------|----------------------|------------------------|----------------|-----------------------|----------------------------|
| Target | 70/100 | 85/95 | 2500/2600 | 40/60 | | 1.00 | | 4.35/4.60 | | | 70000 | 100000 | 3.0 | | |
| 1.01 | 70 | 94 | 2630 | 39.4 | 19 | 1.01 | D200129 | 4.32 | 1.27 | 83.5 | 59672 | 111618 | 5.9 | 1007901 | 236 |
| 1.02 | 100 | 86 | 2590 | 39.4 | 20 | 1.03 | | 4.32 | 0.90 | 83.9 | 59067 | 111690 | 6.1 | 969592 | 248 |
| 1.03 | 70 | 87 | 2490 | 39.4 | 15 | 1.01 | | 4.32 | 1.83 | 83.9 | 59353 | 111045 | 5.6 | 1052980 | 251 |
| 1.04 | 100 | 95 | 2470 | 39.4 | 18 | - | | 4.32 | | | | | | | |
| 1.04r* | 100 | 95 | 2390 | 38.2 | 13 | 1.01 | D200506 | 4.37 | 0.39 | 85.3 | 58379 | 105305 | 5.1 | 1150555 | 249 |
| 1.05 | 70 | 89 | 2660 | 38.7 | 16 | 1.03 | D200206 | 4.68 | 1.05 | 87.0 | 60592 | 103267 | 4.1 | 1474354 | 250 |
| 1.06 | 100 | 95 | 2620 | 38.7 | 17 | 0.99 | | 4.68 | 1.68 | 83.7 | 65341 | 110610 | 5.4 | 1217842 | 252 |
| 1.07 | 70 | 97 | 2510 | 38.7 | 19 | 1.03 | | 4.68 | 1.42 | 84.7 | 65014 | 107984 | 4.9 | 1321837 | 250 |
| 1.08 | 100 | 84 | 2460 | 38.7 | 13 | 1.02 | | 4.68 | 1.11 | 80.5 | 64257 | 100584 | 3.9 | 1627148 | 254 |
| 1.09 | 70 | 86 | 2660 | 56.0 | 16 | 0.98 | D200225 | 4.48 | 1.10 | 81.9 | 64194 | 109214 | 5.5 | 1157565 | 252 |
| 1.10 | 100 | 95 | 2630 | 56.0 | 24 | 0.99 | | 4.48 | 0.23 | 77.6 | 61128 | 109776 | 5.3 | 1150022 | 257 |
| 1.11 | 70 | 95 | 2520 | 56.0 | 18 | 1.03 | | 4.48 | 1.09 | 77.0 | 61960 | 112999 | 5.8 | 1062280 | 257 |
| 1.12 | 100 | 87 | 2470 | 56.0 | 13 | 0.94 | | 4.48 | 1.54 | 78.1 | 60275 | 106168 | 4.9 | 1238779 | 259 |
| 1.13 | 70 | 95 | 2620 | 58.2 | 17 | 0.99 | D200318 | 4.63 | 1.04 | 79.2 | 63752 | 106849 | 5.2 | 1225381 | 263 |
| 1.14 | 100 | 86 | 2530 | 57.4 | 14 | - | | 4.59 | | | | | | | |
| 1.14r* | 100 | 87 | 2540 | 58.2 | 14 | 0.99 | D200508 | 4.64 | 1.53 | 75.6 | 64080 | 109605 | 5.8 | 1097876 | 258 |
| 1.15 | 70 | 85 | 2450 | 58.2 | 14 | 1.00 | D200318 | 4.63 | 1.23 | 78.0 | 65060 | 110863 | 5.5 | 1179624 | 265 |
| 1.16 | 100 | 95 | 2420 | 58.2 | 14 | 0.95 | | 4.63 | 0.39 | 80.6 | 65210 | 110327 | 5.1 | 1272226 | 265 |

DOE #2 RESULTS

All test castings, step plates as well as finger plates, were sectioned for various measurements per the sectioning layout as shown in Figures 11 and 14. Figure 17 is one of the outputs showing hardness as a function of the various combinations of section thickness and mold materials for the vertically-parted finger test plates. Figure 18 shows similar results for the step plate.

SHRINKAGE META MODELING (G10S METAMODEL)

The experimental data from the controlled laboratory trials as well as simulation data, report shrinkage volume after casting. In contrast, the historical data only reported a shrinkage percentage within a casting campaign, without a one-to-one correlation of individual processing conditions and shrinkage. To make the most use of all available data, it was combined, and the modeling of shrinkage was treated as a classification task (i.e., the model predicts whether shrinkage will occur or not, along with a

probability of shrinkage, p_s , which indicates the confidence for the prediction).

For the historical data, the mean value of predictors for one campaign was taken as a single data point, with the occurrence of shrinkage as a response, totaling 33 data points. For the new experimental and simulation data, the volume fed was converted to a binary shrinkage indicator based on an empirical threshold. The missing values were recovered using mean imputation (MI) as introduced previously. In total, there were 69 data points for 27 predictors.

Preliminary variable selection and verification were performed first. A decision tree model was trained and found that only carbon equivalent (CE) was selected by the model (Figure 19). The effect plot in Figure 19 (b) does not clearly show whether CE's effect is linear. However, CE was not included in the final meta-model as a variable; since its individual chemical elements were already incorporated into the model. The Machine Learning (ML) models described here, and that follow are implemented in R programming language unless otherwise specified.

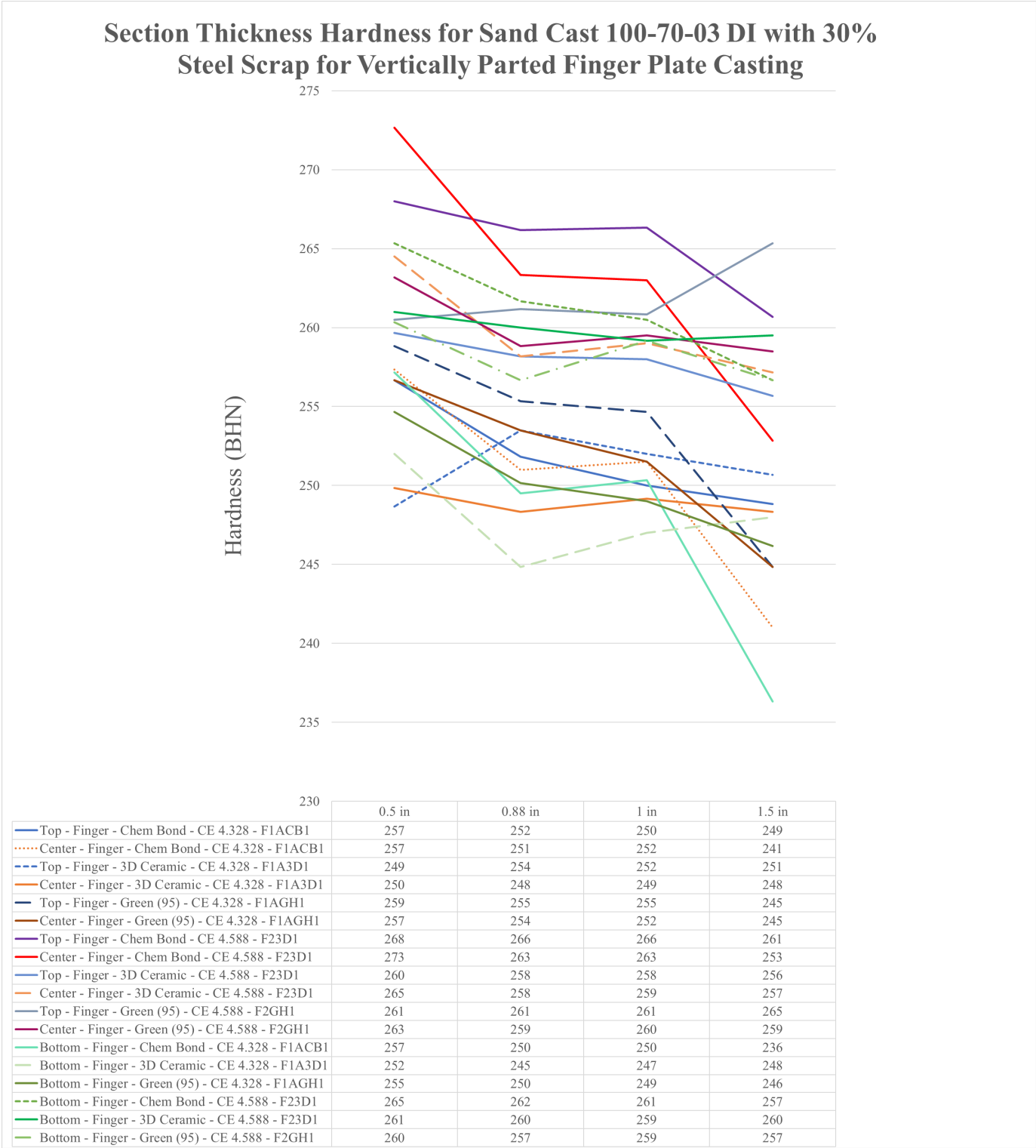


Figure 17. Hardness in various section thickness of vertically-parted finger test castings in various mold materials.

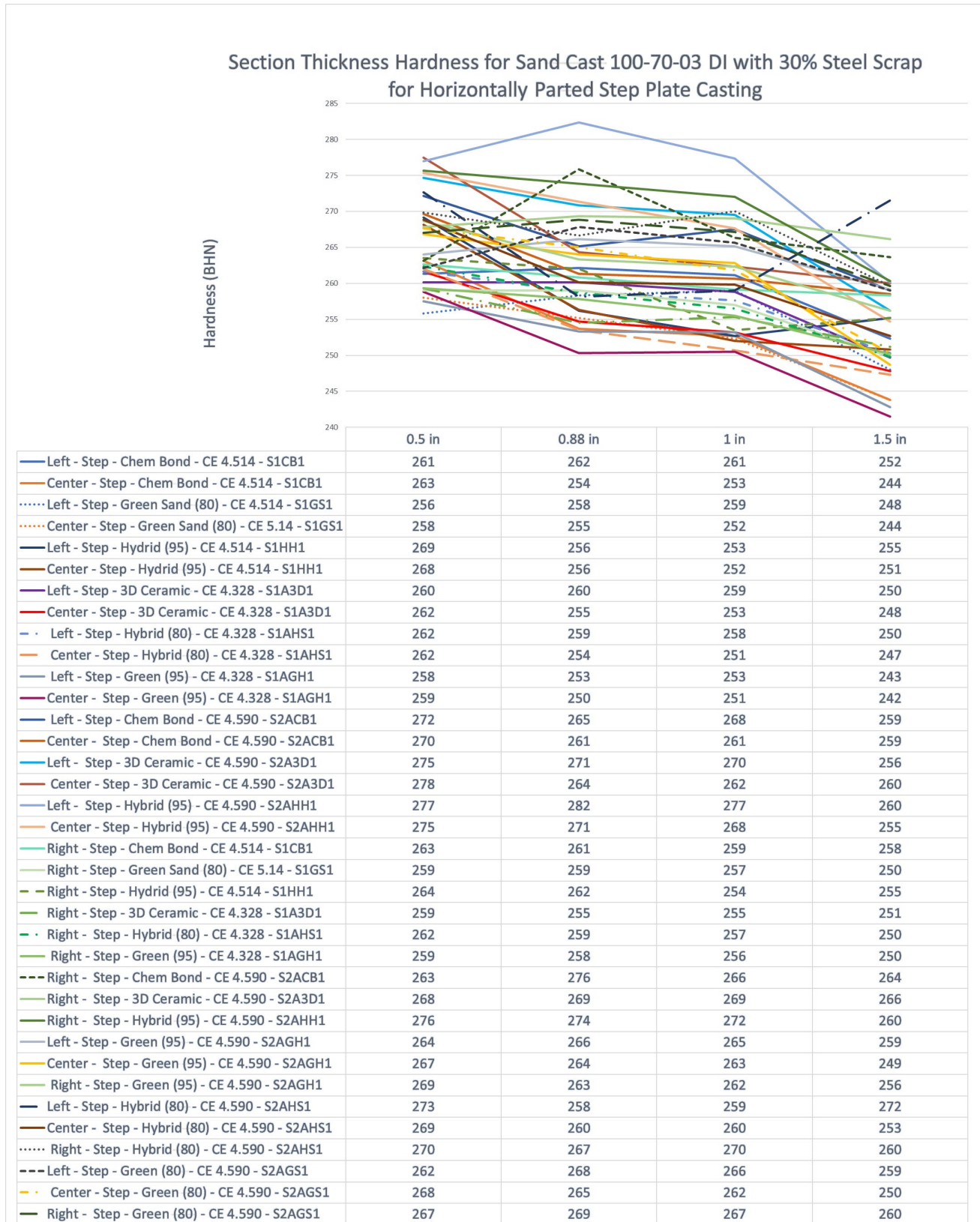


Figure 18. Hardnesss in various section thicknesses of horizontally-parted step test castings in various mold materials.

Secondly, a gradient boosting model was trained, from which a variable importance quantification was obtained as shown in Figure 20 (a), which guides variable selection. The variables' effects were investigated using ALE (Accumulated Local Effects) plots; Figure 20 (b) shows an example of alloy factor. There appears to be a cutoff value, across such value the outcome changes, which indicates that alloy factor has a linear effect except at the cut-off value (4.387). Accordingly, it was determined that most predictors' effects were linear, and it was reasonable to proceed with a linear model.

The elastic net method was used to create a classification model for shrinkage. The two hyperparameters, λ_1 and λ_2 , were tuned using 5-fold

cross-validation (CV) grid search. Note that the hyperparameters are defined differently in the software, but the mathematical meaning is the same. Figure 21 shows some hyperparameter values and resulting performances. Out of the values, the one in red box is selected. It attains an AUC ROC of 0.84.

The sensitivity and specialty values mean the following: out of 100 conditions that lead to shrinkage, 81 will be captured by the model; out of 100 conditions that will not lead to shrinkage, 83 will be predicted correctly as no shrinkage. These metrics suggest that the model has a high reliability.

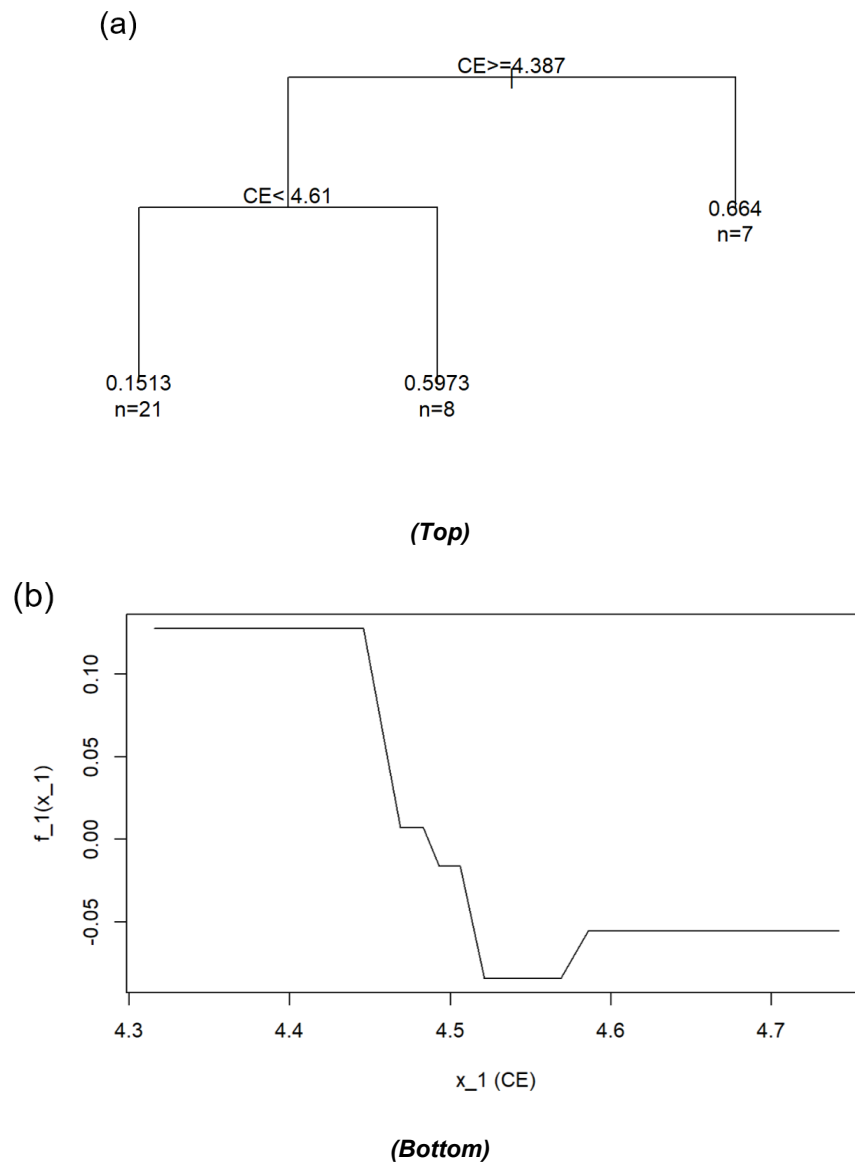


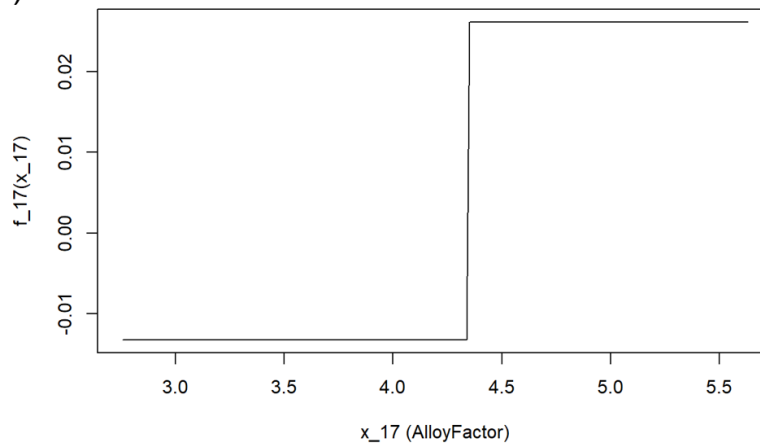
Figure 19. Decision tree model for shrinkage: (a) separation points and (b) effect of CE.

(a)

| | var <chr> | rel.inf <dbl> |
|-----------------|-----------------|------------------|
| Al.wt | Al.wt | 20.022012 |
| CE | CE | 18.092439 |
| P.wt | P.wt | 14.452492 |
| C.wt | C.wt | 10.324482 |
| Si.wt | Si.wt | 10.021117 |
| Cu.wt | Cu.wt | 6.379582 |
| V.wt | V.wt | 5.073832 |
| Sn.wt | Sn.wt | 4.792553 |
| PourTemperature | PourTemperature | 4.527615 |
| Mg.wt | Mg.wt | 3.671029 |

(Top)

(b)



(Bottom)

Figure 20. Results of gradient boosting model for shrinkage: (a) relative variable importance, and (b) ALE plot for alloy factor.

| alpha | lambda | ROC | Sens | Spec |
|-------|--------------|-----------|-----------|-----------|
| 0.1 | 0.0001423759 | 0.6514456 | 0.5666667 | 0.6428571 |
| 0.1 | 0.0003289068 | 0.6556122 | 0.5666667 | 0.6428571 |
| 0.1 | 0.0007598174 | 0.6720238 | 0.5380952 | 0.6428571 |
| 0.1 | 0.0017552769 | 0.6926020 | 0.6000000 | 0.6678571 |
| 0.1 | 0.0040549174 | 0.7474490 | 0.6571429 | 0.6964286 |
| 0.1 | 0.0093673853 | 0.7723639 | 0.6619048 | 0.7250000 |
| 0.1 | 0.0216398756 | 0.8021259 | 0.7238095 | 0.7500000 |
| 0.1 | 0.0499909206 | 0.8240646 | 0.7571429 | 0.8035714 |
| 0.1 | 0.1154855133 | 0.8488095 | 0.8142857 | 0.8321429 |
| 0.1 | 0.2667865208 | 0.8446429 | 0.8142857 | 0.8321429 |
| 0.2 | 0.0001423759 | 0.6329932 | 0.5666667 | 0.6428571 |
| 0.2 | 0.0003289068 | 0.6514456 | 0.5666667 | 0.6428571 |
| 0.2 | 0.0007598174 | 0.6720238 | 0.5380952 | 0.6428571 |
| 0.2 | 0.0017552769 | 0.6926020 | 0.5666667 | 0.6678571 |

Figure 21. Part of the hyperparameter values tested in the grid search, along with the ROC, sensitivity, and specialty of the resulting models.

AS-CAST YIELD STRENGTH META MODELING (G10Y METAMODEL)

The modeling of as-cast yield strength (σ_Y) followed a very similar procedure. At first, data was cleaned and combined. Then, several Machine Learning (ML) models were tested, and variables selected. Unique aspects were: (1) unlike shrinkage, predicting σ_Y was a regression problem since the response takes a continuous value. (2) σ_Y was mostly dependent on chemistry but less related to processing conditions, therefore, only chemistry-related predictors were included. (3) Predictors may have interactions in affecting σ_Y . Given these, a linear model involving first-order interactions was used. The model was trained using a stepwise linear regression technique: predictors were added to/removed from the model step-by-step, until an optimal-performing model was obtained. In the end, a model was trained with CV $R^2 > 0.85$.

All the historical data on the properties are from the 1" section thickness standard test bar, cast separately using no-bake molds. However, some processing conditions (e.g., section thickness, mold material, and orientation) were found to be also impactful on σ_Y , but not included in the original model. These variables were not available in the historical data, but only recorded in some of the new data sets. For these variables, another linear model was trained to get the coefficients measuring their effects on σ_Y . We then

added correction terms for them in the original model, while updating the model's intercept. This keeps the model outcome unchanged when these variables take the same values as in the historical data.

PRODUCTION TRIAL AT FOUNDRY A

The demonstration part production trials at Foundry A entailed four treatment ladles (two for as-cast yield strength metamodel validation and two for shrinkage metamodel validation) and poured 40 experimental casting molds along with 160 regular production molds/castings. Experimental data was collected for mold hardness, regular production-generated sand properties, riser sleeve compressions, pour temperatures, pour times, and both initial and final chemistries. Forty experimental molds were serialized to get a one-to-one relationship, permitting verification. Test bars were poured with the final chemistry for all four ladles. The final composition and mechanical properties were determined both by the foundry internally as well as by an independent, third-party laboratory. The castings from the shrinkage metamodel validation lots were 100% X-rayed to confirm internal shrinkage in addition to being visually inspected for any shrinkage at the riser connection, as is typically done in regular production in the past. Figure 22 captures a pictorial summary of the production trials at Foundry A.

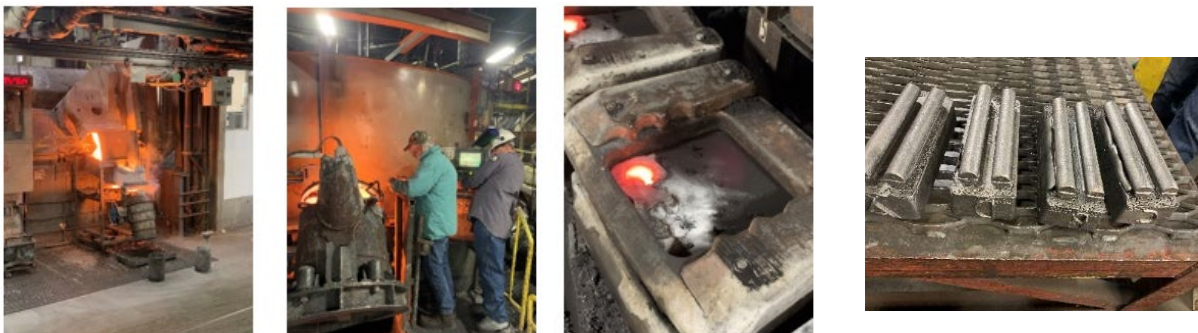


Figure 22. Foundry A production trial photos, from left: transfer ladle; auto pour ladle with adjustments; production mold; and the cast test bars.

Prior to ladle filling, chemistry data was entered into the metamodels to predict as-cast yield strength. The first two ladles (ladles #1 and #2) were purposely designed to predict lower than desired as-cast yield strengths. Subsequently, corrective actions using an additive strategy (e.g., elemental additions which directly impact the as-cast yield strength positively) were determined by using the metamodel and enacted

by making the weighed-out additions into the auto pour ladle. Samples from these experimental ladles were poured into test molds and test bars for evaluation. Similar trials were performed in ladles #3 and #4 to validate the shrinkage metamodel. Figure 23 displays the laboratory setup for the production trials. Figure 23 (left view) show the Excel-driven metamodel running on a laptop in the laboratory next

to the spectrometer. During this stage, the initial chemistry was entered into the metamodel (a lower as-cast yield strength was predicted in these cases) and then a corrective action plan was computed using the metamodel to add specific elemental additions. These elemental additions were pre-weighed (Figure 23, middle view) and then the additions were added to the auto pour. This entire exercise was complete in less than 2 minutes with the metamodel predictions and correction results being processed in only a few seconds.

Figure 24 demonstrates a typical snapshot of the input-output of the G10Y metamodel that was used at Foundry A during the production trials. The predicted as-cast yield strength of 74 ksi compares favorably against both the actual internally measured value of 72 ksi as well as the 74 ksi measured by an independent, third-party laboratory.

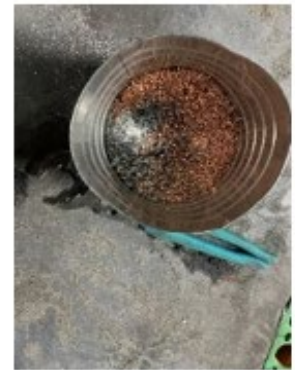
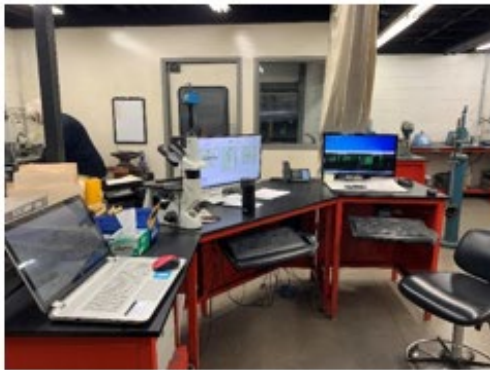


Figure 23. Metamodeling demonstration near real time corrective actions; (left) Excel file drive metamodel in the laboratory next to the spectrometer for quick data access and entry; (middle) weighed corrective additions in the laboratory; (right) corrective additions at the auto pour.

Figure 25 demonstrates a typical snapshot of the input-output of the G10S metamodel that was used at Foundry A during the production trials. In this screenshot, the model predicted no shrinkage to a probability confidence of 0.70; a prediction

seemingly validated when the production trial did not produce any visual shrinkage scrap. For further validation, the subject castings were also submitted to a third-party laboratory for X-ray evaluation that confirmed the lack of shrinkage.

Please input the final chemistry values below the highlighted cells. They must be within the min/max range of the training data.

| | | | | | | | | | | | | | | | | |
|------------------------------------|--------|---|-------|-------|------|-------|-------|-------|-------|-------|-------|-------|-------|-------|-----------|--|
| PREDICTION | | | | | | | | | | 0.075 | 0.014 | 0.9 | | | | |
| Yield = 74518.263 | | Actual | 73583 | | | | | | | | 74740 | 75073 | | | | |
| *Use this prediction with caution. | | | | | | | | | | | | | | All 3 | 77 Zn | |
| | | | | | | | | | | | | | | Al | 75.1 Zr | |
| Positive coefficient. Higher value | | | | | | | | | | | | | | Mo&Cu | 76.3 both | |
| Zero coefficient. | | | | | | | | | | | | | | Cu | 75.1 Ti | |
| Negative coefficient. Lower value | | | | | | | | | | | | | | FeMo | 76.3 Ni | |
| | | | | | | | | | | | | | | Base | 74.4 | |
| for testing: | FinAF1 | FinFe | RevSi | FinMn | FinP | FinS | FinCr | FinMo | FinNi | FinAl | FinCo | FinCu | FinMg | FinNb | FinTi | |
| | 1.217 | 92.4 | 2.447 | 0.46 | 0.02 | 0.012 | 0.048 | 0.024 | 0.036 | 0.008 | 0.007 | 0.851 | 0.038 | 0.008 | 0.008 | |
| expected: | Yield | % error from expected (if using the "for testing" only) | | | | | | | | | | | | | | |
| | 73583 | 1.34265 | | | | | | | | | | | | | | |

(Top)

| | | | | | | | | | | | | |
|-------|-------|-------|---------|-------|-------|-------|-------|--------|---------|-------|---------|-------------------------|
| 5 | 5 | | 6 | 2 | | 1 | | | | | | |
| FinV | FinPb | FinSn | FinB | FinZr | FinAs | FinZn | FinCE | MainAF | Calc Fe | Sb | CE | Calculated Alloy Factor |
| 0.006 | 0.001 | 0.004 | 0.0001 | 0.002 | 0.002 | 0.002 | 4.524 | 4.3872 | 92.389 | 0.002 | 4.48331 | 5.2036 |
| | | | too low | | | | | | | | | |
| 0.002 | 0.001 | | 0.0002 | 0 | | 0.001 | | | | | | |
| 0.01 | 0.006 | | 0.0021 | 0.007 | | 0.008 | | | | | | |
| 70.6 | | 76 | | | | | | | | | | |
| 72.7 | | 74.6 | | | | | | | | | | |
| 73.5 | | 74.9 | | | | | | | | | | |
| 73.6 | | | | | | | | | | | | |
| 74.3 | | 74.8 | | | | | | | | | | |
| 74.4 | | | | | | | | | | | | |
| FinV | FinPb | FinSn | FinB | FinZr | FinAs | FinZn | FinCE | MainAF | | | | |
| 0.006 | 0.005 | 0.008 | 0.0008 | 0.004 | 0.011 | 0.002 | 4.524 | 4.3872 | | | | |

(Bottom)

Figure 24. Typical input and output of the G10Y model during production trials at Foundry A. The top view shows the left-hand side of the spreadsheet model while the bottom view shows the right-hand side.

| | | | | | | | | | | | | |
|---|---|--|----------|-------------|----------|----------|----------|----------|-------|----------|----------|------|
| Please input the chemistry and processing conditions below. | | | | | | | | | | | | |
| Note: outside of the min-max range will lead to extrapolation, for which reliability is not guaranteed. | | | | | | | | | | | | |
| Predictors | 5 | 6 | | 8 | 7 | 7 | 3 | | 5 | | 1 | |
| | MoldHardness | SleeveCompression | CE | urTemperatu | PourTime | MeltC | RevSi | FinMn | FinCu | FinMg | FinP | |
| Value | 95 | 100 | 4.564679 | 2550 | 12 | 3.744621 | 2.472448 | 0.398103 | 0.847 | 0.050172 | 0.015103 | |
| Min | 85.00 | 70.00 | 4.07 | 2390.00 | 12.20 | 3.52 | 1.78 | 0.40 | 0.30 | 0.00 | 0.01 | |
| Max | 95.00 | 100.00 | 4.74 | 2660.00 | 24.00 | 3.88 | 2.92 | 0.54 | 1.01 | 0.07 | 0.02 | |
| | | | | | | | | | | | | |
| Shrinkage | Probability | Probability --> confidence of shrinkage prediction being correct | | | | | 2.472448 | 0.847 | | | | |
| N | 0.70 | | | | | | 2.7 | 0.9 | | | | |
| | | | | | | | | | | | | |
| | | | | | | | | | | V | 0.61 | |
| | | | | | | | | | | Sn | 0.69 | |
| | | | | | | | | | | Ptemp | 0.68 | |
| | Positive coefficient. Higher value --> shrinkage more likely. | | | | | | | | | | Al/Cu | 0.51 |
| | Zero coefficient. | | | | | | | | | | Cu | 0.69 |
| | Negative coefficient. Higher value --> shrinkage less likely. | | | | | | | | | | Al | 0.51 |
| | | | | | | | | | | N | 0.7 | |

(Top)

[illegible]

(Bottom)

Figure 25. Typical input and outputs of the G10S model during production trials at Foundry A. The top view shows the left-hand side of the spreadsheet model while the bottom view shows the right-hand side.

PRODUCTION TRIAL AT FOUNDRY B

Before running the production trials, the worst and best conditions with respect to the X-ray internal soundness levels were simulated using an ICME-

based process simulation and correlated with actual results as shown in Figure 26. Level 2 is acceptable for the second demonstration military part made by Foundry B.

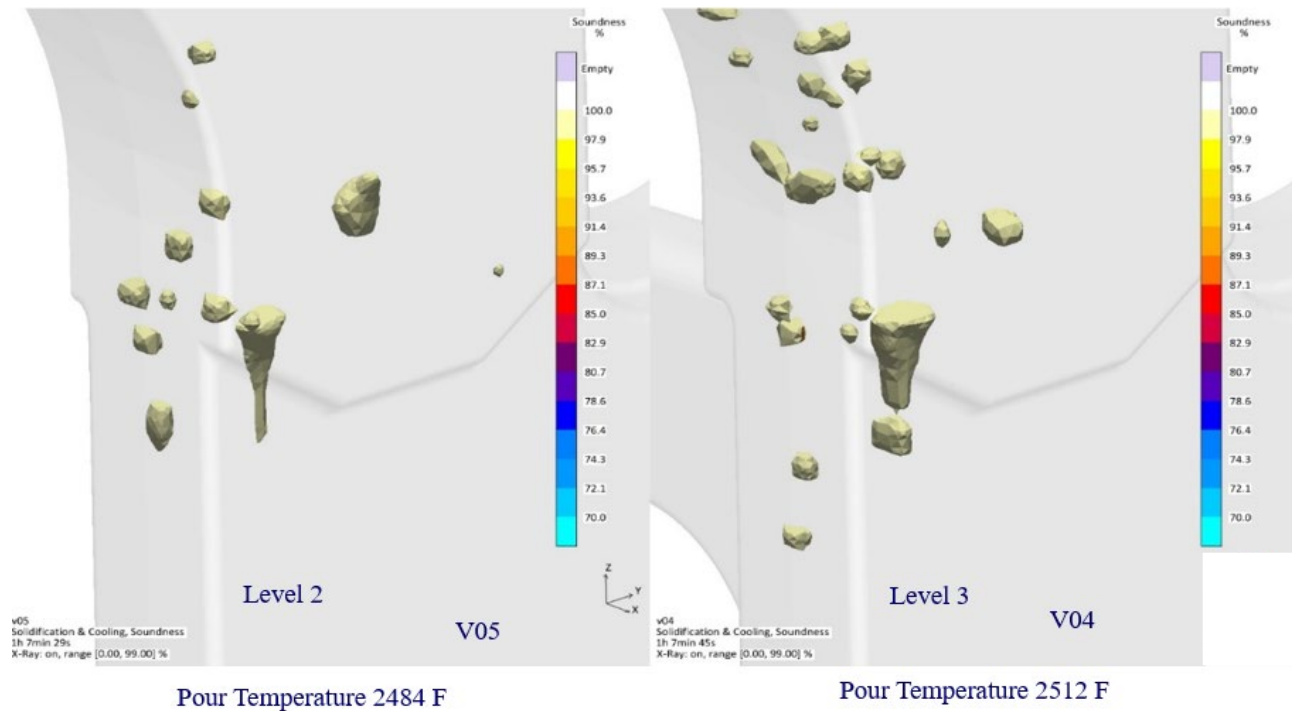


Figure 26. Foundry B demonstration military part ICME-based assessment using metamodel outputs.

Some potential adjustments and corrective actions were pondered based on the historical data mining assessment and recent final chemistries. Both additive (additions to improve a property) and a subtractive strategy (reduced to improve a property) were considered in order to predict and achieve Level 2 shrinkage soundness probability using the G10S metamodel. A typical output for the G10S model is shown in Figure 27. A verification trial was run for this batch of demonstration parts using the metamodel recommended outputs (e.g., lower Al, increasing Si, and a lower pour temperature). The pour temperature was lowered by merely holding the pouring ladle for some time until it cooled. True to prediction, a Level 2 was achieved in all parts produced.

METAMODELING-RELEVANT

Following are the recommendations from this work in selecting an appropriate model for a problem, which may be helpful in other materials informatics studies.

- Linear model is preferred when appropriate. If the predictor–response relation is known or found to be linear, then linear regression (maybe with extensions) is most proper because of its simplicity and interpretability.
- Lasso model and decision trees are useful for variable selection. They may be used to select linearly and nonlinearly important variables,

respectively, guiding the training of more complicated models.

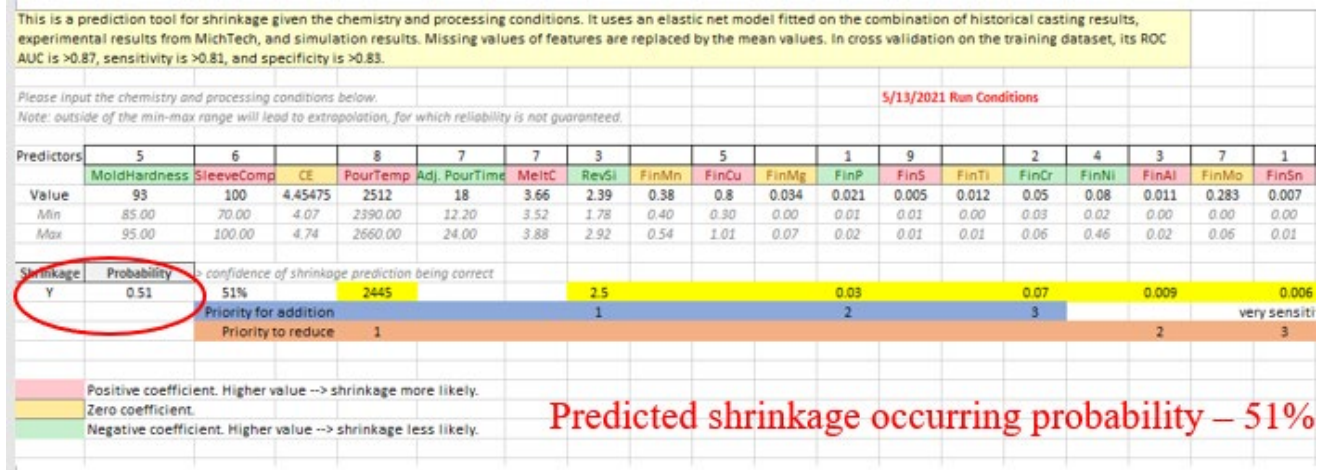
- With sufficient data, ensemble models are likely to perform well. Once an ensemble model with high accuracy is obtained, methods such as Accumulated Local Effects (ALE) plots may be used to extract variable importance and effect information. Such information may guide the choice of a simpler, more interpretable model.
- When uncertainty quantification is desired, for example, in Bayesian Optimization (BO)⁶ scenario, Gaussian Process (GP) models are likely to fulfill the need. There are extensions to GP models that allow modeling mixed numerical and categorical variables,⁷ handling large data,⁶ and physics-informed Machine Learning (ML).⁸

PRODUCTION TRIALS-RELEVANT

In order to accurately predict the final chemistry, the chemistry of the metal in the ladle before pouring needs to be accurate. The approach we used and recommended is to use the final preliminary chemistry and accurately account for all the additions with known recovery, for example of C, Si, and other key elements including trace elements impacting as-cast yield strength and shrinkage tendency. Then, the adjusted chemistry reading should be entered into the metamodel for predicting the desired

response variable—as-cast yield strength or shrinkage probability. Based on the outcome, corrective actions should be computed with additive strategy since subtractive strategy is often not practical. The subtractive strategy can be applied for the subsequent heats to achieve the desired outcome with fine adjustments with

metamodels. Based on the impact of some of the trace elements, all the charge additions including the scrap and returns must have the detailed chemical analysis and % recovery known. DOE #3 was undertaken to provide further clarification on this aspect.



(Top)

- Subtractive strategy – parameters in **Pink** need to be lowered for lower shrink.
 - Al (drop from 0.011 to 0.009 %)
 - Sn (drop from 0.007 to 0.006 %)
 - V(drop from 0.014 to 0.009 %)
 - pour temperature from 2512 to 2445 F
- Additive strategy – parameters in **green** need to be increased to lower shrink.
 - Si (can we increase to 2.5%?)
 - P (can we increase to 0.03%?)
 - Cr (can we increase to 0.07%?)

(Bottom)

Figure 27. G10S Metamodel-based prescriptive recommendations for the production trials at Foundry B. Top is metamodel spreadsheet output, bottom is list of strategies for resolution.

SUMMARY OF WORK WITH CONCLUSIONS

- Proposed a metamodel-based intelligent casting manufacturing approach to solve sporadic quality problems require all the process-related data including detailed chemistry with trace elements to be captured and available digitally from various areas. The data needs to be mined and arranged chronologically.
- The proposed methodology and framework are applicable to solve any casting quality problems driven with uncertainty but will require some controlled DOEs to generate more data to quantify the uncertainty for accurate predictions.
- Metamodels for the same grade and molding process have been demonstrated to work universally, independent of the production foundry location, in this case for 100-70-03 grade ductile iron sand castings.
- Matured ICME-based process modeling is very valuable in metamodel development, especially with surrogate model building, model calibration, validation, and verification. These ICME-based process models provide additional data sets to make the metamodels more robust and accurate.

- In this Excel sheet, the tradeoff between higher strength and lower yield probability are indicated for each variable. This allows users to fine tune the casting settings towards optimizing performance (σ_y , in this case) to avoiding shrinkage. Compared to optimization algorithms such as linear programming, this approach provides more flexibility (not restricted to a single optimal solution) and tolerance to model inaccuracy (which is unavoidable for computational models).

(Top)

(Bottom)

Figure 28. Screenshot of the Excel tool for shrinkage prediction. Top view is the left-hand side of model spreadsheet while the bottom is the right-hand side of model spreadsheet.

(Top)

(Bottom)

Figure 29. Screenshot for the Excel tool for optimizing σ_y and shrinkage concurrently. The top view shows the left-hand side of the spreadsheet model while the bottom view shows the right-hand side.

- DOE #1-based conclusions: higher pour temperature, soft mold and risers sleeve compressed to 100%, higher steel scrap in the furnace charge; all lead to higher shrinkage in 100-70-03 sand cast ductile irons.
- DOE #2-based conclusions: as-cast yield strength in 100-70-03 grade of sand cast ductile iron decreases with an increase in the section thickness of the casting. Vertical features with respect to gravity show lower values marginally than horizontally oriented features.
- The G10Y metamodel shows that for 100-70-03 ductile iron sand castings, chemical elements Mo, Al, Cu, Mg, V and B have a positive impact on as-cast yield strength (meaning, the higher the values, the higher the as-cast yield strength); whereas Ni, Ti, P, Zn and Zr have a negative impact on the as-cast yield strength (meaning the higher the values, the lower the as-cast yield strength).
- The G10S metamodel shows that for 100-70-03 ductile iron sand castings, key process parameters are—mold hardness (softer mold, more shrinkage), pour temperature (higher temperature more shrinkage), riser sleeve compression (100% more shrinkage than 70% compressed); chemical elements C, S, Al, Cu, Mo, V, & Sn have a positive impact meaning the higher the values, the more shrinkage occurring tendency, whereas elements Si, P, Ni, Cr, Zn have a negative impact, meaning, the higher values will reduce the shrinkage tendency.
- The G10YS metamodel additionally provides as-cast yield strength dependency on the section thickness (heavier section thickness, lower the value); casting orientation (horizontal provides slightly higher strength than vertically oriented) and mold material type (properties lower in the order as 3D printed ceramic, chemically bonded silica, and then green sand) and estimates the shrinkage probability simultaneously.
- The metamodels developed are indicative of the impact of some of the trace elements on as-cast properties and shrinkage tendency in 100-70-03 grade of ductile iron sand castings—Al, B, V, Zn, Zr, Pb, Ti.
- Further research is needed to quantify the various sources contributing to the trace elements levels observed in the final chemistry. Potential sources for the trace elements that might need better control include, but are not limited to: scrap, pig iron, ferroalloys, treatment alloys and inoculants. Additionally, the Spectro analyzer detection limits and sensitivity, along with possible contamination from the sample preparation (i.e., polishing abrasives and methods for cutting the samples), may have impacted the trace element readings. Further research is also advised to better understand the mechanism triggering either increases or decreases in the yield strength, for example, impact on the metal matrix composition (% ferrite, % pearlite, % graphite, carbides, etc.).
- Production trials were demonstrated in near real-time. The G10Y and G10S metamodels were used to assess the situation in real time after plugging in all the input data, which then based on the model predictions (in a fraction of seconds), corrective actions were taken to salvage the lot(s). These metamodel-derived corrective actions ended up producing shrinkage-free castings meeting the minimum as-cast yield strength requirements for the demonstration military parts. The metamodels developed are embedded into an Excel file and are very easy to use, while not requiring expensive third-party software.
- Metamodels can be used to optimize the chemical composition by reducing expensive alloying elements like Ni, Mo, and Cr; keeping them on the lower side, thereby relieving some of the supply chain strains currently being experienced in the industry.
- G10YS Metamodel can be used by the design engineer to predict the as-cast properties and shrinkage tendency in various areas of the casting geometry for 100-70-03 grade of sand cast ductile iron as a function of section thickness, chemical composition, orientation of the feature, mold hardness and type of mold binder intended to be used.
- Please note the accuracy of the meta-models is limited to the data provided and near data extrapolations, but not extremes. Its accuracy will be lost if worked outside of the chemistry and process ranges.

ACKNOWLEDGMENTS

This AMC project was sponsored by the Defense Logistics Agency-Troop Support, Philadelphia, PA and the Defense Logistics Agency Information Operations, J68, Research & Development, Ft. Belvoir, VA. The authors are grateful for the support from the late Mr. Steve Robison, AFS, and the AFS corporate member production foundries for providing the required data and conducting production trials for metamodel validation and verification. The authors acknowledge the support from academic institutions towards AI/ML technology and laboratory-controlled DOE-based casting trials.

REFERENCES

1. Shah, Jiten, Chan, Wei, Olson, Greg, et al., "Data-Driven Prediction of Mechanical Properties in Support of Rapid Certification of Additively Manufactured Alloys," *Computer Modeling in Engineering and Sciences*, Volume 117 (2018). (MxD/DMDII project outcome).
2. Sobol, I.M., "On the distribution of points in a cube and the approximate evaluation of integrals," *USSR Computational Mathematics and Mathematical Physics*, 7(4) pp. 86-112 (1967).
3. Li, W.W. and Li, C.F., Wu, Jeff, "Columnwise-Pairwise Algorithms With Applications to the Construction of Supersaturated Designs," *Technometrics*, 39(2), pp. 171-179 (1997).
4. Jin, R., Chen, W., and Sudjianto, A., "An efficient algorithm for constructing optimal design of computer experiments," *Journal of Statistical Planning and Inference*, 134(1), pp. 268-287 (2005).
5. Tibshirani, R., "Regression Shrinkage and Selection via the Lasso," *Journal of the Royal Statistical Society, Series B (Methodological)*, 58(1) pp. 267-288 (1996).
6. Hilt, D.E., et al., "Ridge, a computer program for calculating ridge regression estimates," Vol. 236 (1977) Upper Darby, Pa: Dept. of Agriculture, Forest Service, Northeastern Forest Experiment Station (1977).
7. Zou, H. and Hastie, T., "Regularization and variable selection via the elastic net," *Journal of the Royal Statistical Society: Series B (Statistical Methodology)*, 67(2) pp. 301-320 (2005).
8. James, G., et al., "An introduction to statistical learning," Springer, Vol. 112 (2013).
9. Breiman, L., "Random Forests," *Machine Learning*, 45(1) pp. 5-32 (2001).
10. Friedman, J.H., "Greedy Function Approximation: A Gradient Boosting Machine," *The Annals of Statistics*, 29(5) pp. 1189-1232 (2001).
11. Apley, D.W. and Zhu, J., "Visualizing the effects of predictor variables in black box supervised learning models," *Journal of the Royal Statistical Society: Series B (Statistical Methodology)* 82(4) pp. 1059-1086 (2020).
12. Rasmussen, C.E. and Williams, C.K.I., "Gaussian Processes for Machine Learning," *Adaptive Computation and Machine Learning Series*, Cambridge, Massachusetts: MIT Press (2005).
13. Arendt, P.D., Apley, D.W., and Chen, W., "Quantification of Model Uncertainty: Calibration, Model Discrepancy, and Identifiability," *Journal of Mechanical Design*, 134(10) Article number #100908 (2012).
14. Sacks, J., Schiller, S.B., and Welch, W.J., "Designs for Computer Experiments," *Technometrics*, 31(1) pp. 41-47 (1989).
15. Zhang, Y., Apley, D.W., and Chen, W., "Bayesian Optimization for Materials Design with Mixed Quantitative and Qualitative Variables," *Scientific Reports*, 10(1) pp. 4924 (2020).
16. Kennedy, M.C. and O'Hagan, A., "Bayesian calibration of computer models," *Journal of the Royal Statistical Society: Series B (Statistical Methodology)*, 63(3) pp. 425-464 (2001).